CHAPTER 7

Different theoretical approaches in the study of antioxidative mechanisms

Contents

Computational Modeling in Bioengineering and Bioinformatics
ISBN 978-0-12-819583-3, DOI: 10.1016/B978-0-12-819583-3.00007-2

1 PREVENTION OF OXIDATIVE STRESS

Although oxygen is crucial for aerobic organisms, it also represents one of the main intergradients for the production of the reactive oxygen species (ROS) (Augustyniak et al., 2010). Free radicals and other reactive species are constantly generated in the human body. Oxidative stress (OS) is caused by an imbalance between the production of ROS and ability of biological systems to readily detoxify the reactive intermediates or easily repair the resulting damage. OS has been proposed to play an important role in the pathogenesis of many (if not all) diseases, such as inflammation, cancer, hypertension, cardiovascular disease, diabetes mellitus, atherosclerosis, ischemia/reperfusion injury, neurodegenerative disorders, rheumatoid arthritis, and ageing (Halliwell and Gutteridge, 2015; Fridovich, 1978; Sies, 1997; Thomas, 1998; Halliwell, 2005). The organisms have developed a variety of the internal defense mechanisms that include endogenous enzymes (such as superoxide dismutase and catalase), copper and iron transport proteins, and water-soluble and lipid-soluble antioxidants to counteract the damaging effect of free radicals. Also, there are some external factors including dietary substances (flavonoids, phenolic acids, vitamins C and E, hydroquinones, and various sulfhydryl compounds), which help in the prevention of damage caused by free radical species. All these substances constitute complex antioxidant defense systems.

A possible association between the consumption of foods containing phenolic compounds and a reduced risk of developing disorders, such as cancer and cardiovascular diseases, has been evaluated in several epidemiological investigations (Ness and Powles, 1997; Jacob and Burri, 1996; Block et al., 1992; Huang and Ferraro, 1992). Both natural and synthetic phenolic compounds have been characterized by their antioxidant activity (Rice-Evans et al., 1996; Halliwell et al., 1995; Anouar et al., 2009). Phenolic compounds are plant secondary metabolites commonly found in herbs and fruits. The term phenolics are used for more than several thousands of naturally occurring compounds. One of them is phenolic compounds, which are plant secondary metabolites commonly found in herbs and fruits. The common structural feature of all phenolics is an aromatic ring bearing one or more hydroxyl substituents.

2 CHARACTERISTICS OF GOOD ANTIOXIDANTS IN GENERAL

There are several desirable characteristics that every good antioxidant should have, regardless of their sources. Indeed, even though there are many molecules that show antioxidant properties, not all of them are equally efficient for that purpose. There is a series of requirements proposed, which are helpful in the identification of good antioxidants (Rose and Bode, 1993). They are listed later:

1) Toxicity: Good antioxidant should not be toxic before and after the antioxidant action. In addition, it is also important to be aware of the influence of possible interactions with any drug that may be concurrently consumed.

2) Availability: Antioxidant should be available when needed.

3) Location and concentration: Not only should an efficient antioxidant be present, but also it should be in adequate concentration in cells, due to the fact that most free radicals have short half-lives within biological systems.

4) Versatility: A good antioxidant should be able to easily react with different free radicals, since actually there are a wide variety of them in biological systems.

5) Fast reactions: Based on the many definitions of antioxidants, it is obvious that good antioxidants must react faster with free radicals than the molecules that they protect, and in that way, they can efficiently protect biological targets.

6) Crossing physiological barriers: It is expected that a good antioxidant be able to cross physiological barriers and be rapidly transported into the cells, where it is needed the most.

7) Regeneration: In this context, the term *regeneration* refers to antioxidants that are able to scavenge different free radicals. Antioxidants that have physiological mechanisms that regenerate their original form are expected to be particularly efficient in reducing OS because it is expected that they could scavenge more than one free radical.

8) Minimal loss: The concentration of any chemical compound is reduced in physiological environments by metabolic routes. Therefore, those antioxidants that still possess antioxidant activity

after they undergo metabolic paths are expected to be particularly efficient (e.g., melatonin).

The antioxidative mechanisms can be examined using in silico approaches, such as quantum mechanical calculations. Thermodynamically favorable mechanisms of the action of the investigated molecules can be quantitatively expressed through physicochemical descriptors such as bond dissociation enthalpy (BDE), ionization potential (IP), proton dissociation enthalpy (PDE), proton affinity (PA), and electron-transfer enthalpy (ETE). The transition-state theory (TST) can be applied for the study of the reaction mechanisms in describing the geometry of the corresponding transitional states and calculating the reaction rate constants (k).

However, elucidation of the main reaction mechanisms involved in the antioxidant activities of chemical compounds may be a challenge. For these reasons, some of the most important reaction mechanisms involved in antioxidant protection, in both experimental and theoretical approaches, are investigated in many cases (Ivanović et al., 2016; Petrović et al., 2015). In this chapter, some theoretical results will be presented. For this purpose, quercetin, gallic acid, and dihydroxybenzoic acids are chosen.

Quercetin (Q) is naturally occurring and the most abundant dietary flavonol commonly found in onions, grape, and other vegetables and fruits. According to the DPPH, ABTS, and VCEAC values, as well as structure-activity relationships, quercetin is ranked as one of the most powerful antioxidants in the flavonoid class of compounds (Cai et al., 2006; Kim and Lee, 2004). Constant scientific interest in quercetin arises from its multiple effects on human health including antiviral protection (against parainfluenza virus type 3, herpes simplex virus type 1, and poliovirus type 1), cardiovascular and anticancer protection, inhibition of oxidation of LDL cholesterol in vitro, and inhibitory effects on inflammation-producing enzymes like cyclooxygenase and lipoxygenase, which in their metabolic cycles cause edema, dermatitis, arthritis, gout, and other pathological states. It is found as glycoside in high concentrations in many types of fruits and vegetables (*Ginkgo biloba*, *Hypericum perforatum*, *Sambucus canadensis*, apples, onion, berries, red wine, barks, nuts, flowers, leaves, and seeds) (Cao et al., 1997; Rice-Evans and Miller, 1996; Havsteen, 1983; Bors et al., 1990; Benavente-García et al., 1997; Hertog and Hollman, 1996; Kaul et al., 1985). It has

been shown that quercetin glucosides are hydrolyzed by lactase phlorizin hydrolase (LPH), a β-glucosidase found on the brush border membrane of the mammalian small intestine (pH 7–9). Subsequently, the liberated aglycone can be absorbed across the small intestine (Day et al., 2000; Hollman, 2004; Van Dorsten et al., 2012). The majority of theoretical investigations of Q is focused on all rings where OH groups are located.

Phenolic acids, as hydroxylated derivatives of cinnamic and benzoic acids, bear many functions in plants. One of the compounds from this group is gallic acid (GA). In the plant world, this acid is widely distributed as a free compound, as well as part of hydrolyzable tannins (Bianco et al., 1998). GA can be found in gallnuts, witch hazel, and tea leaves (Pettersen et al., 1993) and also as a part of some hardwood species such as eucalyptus wood (e.g., *Eucalyptus microcrys* f. muell., *E. triantha* link., and *E. regnans* f. muell.) and oak trees (e.g., *Quercus robur*, *Q. alba*, and *Q. rubra*) (Bianco et al., 1998). It is known that GA shows fungicidal and fungistatic properties, as well as strong affinity to form complexes (Koga et al., 1999). Derivatives of gallic acid are biologically active components of other plants and plant products: grape, different berries, fruits, different juices, and wine. GA shows extensive application in medicine, pharmaceutical and chemical industry, and foodstuff, as well as light industry. Because of its good antioxidant properties, GA has great application in medicine in protection of human cells against oxidative damage. Apart from that, GA and its derivatives are particularly effective in treating albuminuria and diabetes, psoriasis and external hemorrhoids, coronary heart disease, cerebral thrombosis, gastric ulcer, snail fever, viral hepatitis, senile dementia, and other diseases where oxidative stress is involved and inhibit insulin degradation (Sakagami et al., 2001). On the other hand, it shows cytotoxicity against cancer cells and antiallergic, antifungal, antiinflammatory, antiseptic, antivirus, and antiasthmatic effects in living organisms.

Dihydroxybenzoic acids (DHBA) as a subclass of hydroxybenzoic acids possess two hydroxyl groups whose mutual position determines their chemical properties. There is some experimental evidence that generally confirms good antioxidant activity of DHBAs (Cai et al., 2006; Kim and Lee, 2004), especially indicating good scavenging potency of 3,4-DHBA and 2,3-DHBA. Protocatechuic acid (3,4-DHBA) is a strong antiradical and antioxidant agent that inhibits the chemical

carcinogenesis and show protection against the hydroperoxide-induced toxicity (De Graff et al., 2003). Also, a few positive health attributes of 3,4-DHBA such as antibacterial (Chao and Yin, 2009), antimutagenic (Stagos et al., 2006), antiinflammatory, anticoagulatory (Lin et al., 2009), and antihyperglycemic (Kwon et al., 2006) actions have been reported. Although all these compounds can be found in natural products, there are certain findings that implicate the nonenzymatic production of 2,3-DHBA (pyrocatechuic acid), which proceeds upon trapping the hydroxyl radical by salicylic acid (Prasad and Laxdal, 1994). Moreover, pyrocatechuic acid may act as a dioxygenases metabolite (Bugg, 2003).

3 THE PROPOSED REACTION MECHANISMS

The scavenging of free radicals seems to play an important role in the antioxidant activity of phenolic compounds. The antiradical properties of phenolic compounds are related to their ability to transfer their phenolic H-atom to a free radical. The reactive radical species ($R^{\bullet}$) in the radical-scavenging mechanisms are inactivated by accepting a hydrogen atom from OH and NH groups of different antioxidants (Ivanović et al., 2016; Petrović et al., 2015). It is known that this reaction proceeds via several mechanisms: hydrogen atom transfer (hydrogen atom transfer [HAT]/proton-coupled electron transfer [PCET], Eq. 7.1), single-electron transfer (SET Eqs. 7.2–7.4), single-electron transfer followed by proton transfer (SET-PT, Eq. 7.5), sequential proton loss electron transfer (SPLET, Eqs. 7.6 and 7.7) sequential proton loss hydrogen atom transfer (SPLHAT, Eqs. 7.8 and 7.9), and radical adduct formation (RAF, Eq. 7.10) (Klein et al., 2007; Litwinienko and Ingold, 2007; Galano, 2015; Galano et al., 2016; Mazzone et al., 2016). These mechanisms may coexist, and they depend on polarity and other properties of solvents as well as on radical characteristics.

3.1 Hydrogen-atom transfer versus proton-coupled electron transfer

Understanding the leading reaction mechanism involved in the antioxidant action is a challenging task. It is well known that reactions ($RXH + X \rightarrow RX + XH$) involving HAT mechanism between two oxygen atoms have much lower activation energies and higher rate

constants than HAT mechanism between two carbon atoms (Min and Boff, 2002).

Mayer and coworkers used the DFT method to examine the self-exchange reactions of the phenoxy radical/phenol, methoxy radical/methanol, and the benzyl radical/toluene systems (Mayer et al., 2002). They identified the geometrical differences in transition states of the HAT and PCET mechanisms. The identification of the transition state was based on the analysis of the singly occupied molecular orbital (SOMO). The HAT mechanism is characterized by a significant SOMO density along the donor ··· H ··· acceptor transition vector. On the other hand, the SOMO of PCET transition state involves *p*-orbitals, which are orthogonal to the transition vector.

In the HAT mechanism, radical species ($R^{\bullet}$) remove a hydrogen atom from the antioxidant molecule (A–OH) that itself converts to a radical ($A–O^{\bullet}$):

$$A–OH + R^{\bullet} \rightarrow A–O^{\bullet} + RH \tag{7.1}$$

This mechanism plays a significant role in the process of analyzing mechanisms of antioxidant activity of different classes of organic compounds, for example, polyphenols, Schiff base, and triazoles. The HAT was proposed as a key reaction mechanism of antioxidative action for different classes of organic compounds, from different literature data (Marković et al., 2014a, b, c; Dimić et al., 2017; Tošović et al., 2017). This mechanism, as mentioned earlier, involves transfer of a proton with one of its bonding electrons.

In the PCET mechanism, the same product is obtained as in the HAT mechanism, but the electron and proton are transferred in a single kinetic step via different routes. The proton is transferred from the phenolic compound to the radical's lone pair, while the electron moves from the 2*p* lone pair of the phenolic compound to the SOMO of phenoxy radical (Rose and Bode, 1993; Mayer, 2004) (Fig. 7.1). It should be pointed out

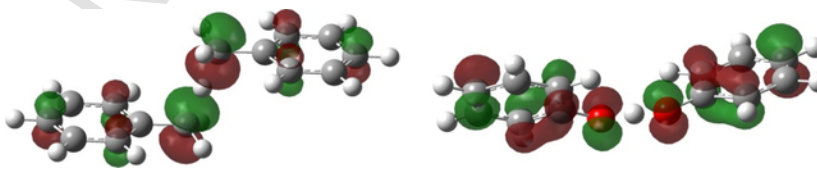

Fig. 7.1 SOMO orbitals in HAT mechanism (*left*) and SOMO orbitals in PCET mechanism (*right*).

that the PCET mechanism is present in many biological and biochemical processes (DiLabio and Johnson, 2007; Mayer et al., 2002).

3.2 Single electron transfer

The SET is the second one-step mechanism, and it can take place following three different pathways:

$$A-OH + {}^{\bullet}R \rightarrow A-OH^{\bullet+} + R^{-} \tag{7.2}$$

$$A-OH + {}^{\bullet}R \rightarrow A-OH^{\bullet-} + R^{+} \tag{7.3}$$

$$A\text{–}O^{-} + R^{\bullet} \rightarrow A\text{–}O^{\bullet} + R^{-} \tag{7.4}$$

Eq. (7.2) has been described as important for the free radical-scavenging activity of the enol isomer of curcumin (Barzegar, 2012) and for the reactions of carotenoids with $^{\bullet}NO_2$ (Mortensen et al., 1997) and $CCl_3OO^{\bullet}$ (Hill et al., 1995), catechin analogs with peroxyl radicals ($ROO^{\bullet}$) (Nakanishi et al., 2004), edaravone derivatives with $^{\bullet}OH$, $^{\bullet}OCCl_3$ and $CH_3COO^{\bullet}$ (Pérez-González and Galano, 2012), and resveratrol with oxygen radicals (Nakanishi et al., 2007). However, the second pathway (Eq. 7.3) is involved in the reactions of the superoxide anion radical ($O_2^{\bullet-}$) with xanthones (Martínez et al., 2012) and carotenoids (Galano et al., 2010) and in the reactions of the NO radical with trolox, caffeic acid, uric acid, and genistein (Sueishi et al., 2011). The relative importance of the second pathway increases with the electron donor capability of the reacting free radical.

3.3 Single electron transfer-proton transfer

The SET-PT mechanism implies two steps. The first step is transfer of an electron to the radical, while the primary antioxidant is transformed into the radical cation (Eq. 7.2). The next step is the heterolytic O–H bond dissociation of $A\text{–}OH^{\bullet+}$ (Eq. 7.5):

$$A\text{–}OH^{\bullet+} + R^{-} \rightarrow A\text{–}O^{\bullet} + RH \tag{7.5}$$

This mechanism is less represented in comparison with the HAT and PCET mechanisms because the first step of this mechanism is very slow. On the other hand, once formed radical cation easily loses one proton in the second step of this mechanism, for example, in the case of baicalein

(Marković et al., 2012a) and quercetin (Marković et al., 2013a, b, c). Furthermore, the SET-PT mechanism plays an important role in the oxidative damage of biomolecules by highly reactive radicals such as hydroxyl radical. For instance, the SET-PT mechanism is the main reaction path for the reaction of the guanosine and hydroxyl radical (Galano and Alvarez-Idaboy, 2009).

3.4 Sequential proton-loss electron transfer

In the SPLET mechanism, antioxidant losses one proton and converts to anion, $A–O^-$ (Eq. 7.6). Further, electron transfer from the antioxidant anion to a radical leads to the formation of the antioxidant radical, $A–O^{\bullet}$, and the corresponding anion R^- (Eq. 7.4), which is further protonated (Eq 7.7):

$$A–OH \rightarrow A–O^- + H^+ \tag{7.6}$$

$$R^- + H^+ \rightarrow RH \tag{7.7}$$

This mechanism is particularly important for the explanation of the antioxidant activity of phenolic compounds under physiological conditions (Foti, 2007). Analyzing the antioxidant activity, two important chemical characteristics of the antioxidant should be mentioned. The first one is its pK_a, which is responsible for the determination of the proportion of the deprotonated species in water solution and at each pH value, for instance, at pH 7.4 (physiological conditions). Moreover, the role of the solvents in these reactions also should not be forgotten. The solvent should be polar and protic and be able to provide good solvation of the formed anion. Therefore, it is expected that the SPLET mechanism is dominant in water, but not in the lipid phase, characteristic of the biological systems. It should be emphasized that the SPLET mechanism has been identified as a crucial mechanism in the scavenging activity exerted by numerous compounds in polar environments.

3.5 Sequential proton loss hydrogen atom transfer mechanism

This mechanism also consists of two steps. The first one is identical to the first step of the SPLET process and yields the deprotonated antioxidant (Eq. 7.8). The second step is completely different compared with SPLET, where instead of the electron transfer, hydrogen atom transfer takes place (Eq. 7.9):

$$A-(OH)_2 \rightarrow A-(OH)O^- + H^+ \tag{7.8}$$

$$A-(OH)O^- + {}^{\bullet}R \rightarrow A-(O^{\bullet})O^- + HR \tag{7.9}$$

As a special mechanistic pathway, SPLHAT mechanism is mentioned in the study of the free radical-scavenging action of anthocyanidins (Estévez et al., 2010). However, its importance in the free radical-scavenging activity for other compounds also has been described. This mechanism is playing a very important role in the reactions of esculetin with $^{\bullet}OOCH_3$ and $^{\bullet}OOCHCH_2$ radicals (Medina et al., 2014) and in the reaction of gallic acid with $^{\bullet}OH$ (Marino et al., 2014). The SPLHAT mechanism is significant for the free radical-scavenging activities of α-mangostin (Martínez et al., 2011), ellagic acid (Galano et al., 2014), propyl gallate, and different phenolic acids (Medina et al., 2013).

Both processes, SPLHAT and SPLET, are mutually competitive, since the first step is common. Therefore, the second step, transferring a hydrogen atom (H) or an electron from the deprotonated antioxidant, plays a very important role in the evaluation of the mechanistic pathway of the action of investigated compound. Accordingly, any factor contributing to the increase in deprotonation (pH, polarity of solvent, reactivity of free radical, etc.) would be in favor of both processes. On the other hand the higher electron donor ability of the deprotonated antioxidant influences the higher probability of SPLET, while species with more labile H atoms would favor the SPLHAT mechanism.

4 RADICAL ADDUCT FORMATION

RAF is a simple mechanism of radical adduct formation between free radical and antiradical species (Eq. 7.10). This mechanism is important for systems containing the π conjugated systems (Galano and Alvarez-Idaboy, 2013; Galano and Francisco-Marquez, 2009). In contrast to the HAT and PCET mechanisms, the antioxidant does not provide its hydrogen atom, but forms the radical adduct with the free radical. This mechanism depends on the structure of the investigated antioxidant and the free radical. If the investigated antioxidant has multiple bonds, then RAF is a possible reaction path. In addition, the properties of the free radical play an important role, and the electrophilic free radicals have the

greatest potential for participation in this type of reactions. Generally speaking the reaction center of the investigated antioxidant should be easily accessible, and a free radical should be small or medium sized to avoid potential steric hindrance:

$$\text{A–OH} + \text{R}^{\bullet} \rightarrow [\text{A–OH–R}]^{\bullet} \tag{7.10}$$

4.1 Thermodynamical parameters for evaluation of antioxidative mechanisms

The most investigated antioxidative mechanisms are HAT, SET-PT, and SPLET. Important thermodynamic parameters that determine dominant mechanisms of free radical scavenging are as follows:

1) Bond dissociation enthalpy (BDE) of A–OH molecule for the HAT mechanism. The importance of BDE is due to the antioxidant activity estimation. The lower BDE value indicates the easier O–H bond rupture.

2) Ionization potential (IP) of A–OH molecule and proton dissociation enthalpy (PDE) of radical cation $\text{A–OH}^{\bullet+}$ for the SET-PT mechanism. The lower value of ionization potential of A–OH indicates easier electron transfers from antioxidant to radical species.

3) Proton affinity (PA) of molecule A–OH and electron energy transfer (ETE) correspondence to anion A–O^{-} for SPLET mechanism.

The reaction enthalpies related to the studied free radical-scavenging mechanisms can be calculated by the following equations (Marković et al., 2012a, b, c; Galano and Alvarez-Idaboy, 2009; Milenković et al., 2017):

$$\text{BDE} = H(\text{A–O}^{\bullet}) + H(\text{H}^{\bullet}) - H(\text{A–OH}) \tag{7.11}$$

$$\text{IP} = H\left(\text{A–OH}^{\bullet+}\right) + H(\text{e}^{-}) - H(\text{A–OH}) \tag{7.12}$$

$$\text{PDE} = H(\text{A–O}^{\bullet}) + H\left(\text{H}^{+}\right) - H\left(\text{A–OH}^{\bullet+}\right) \tag{7.13}$$

$$\text{PA} = H(\text{A–O–}) + H\left(\text{H}^{+}\right) - H(\text{A–OH}) \tag{7.14}$$

$$\text{ETE} = H(\text{A–O}^{\bullet}) + H(\text{e–}) - H(\text{A–O}^{-}) \tag{7.15}$$

where $H(\text{A} - \text{OH})$, $H(\text{A} - \text{O}^{\bullet})$, $H(\text{A} - \text{OH}^{\bullet+})$, $H(\text{A} - \text{O}^{-})$, $H(\text{H}^{\bullet})$, $H(\text{e}^{-})$,

and $H(H^+)$ are the enthalpies of parent molecule, radical, radical cation, and anion of the examined compound, hydrogen atom, electron, and proton, respectively. For calculation of the mentioned thermodynamical parameters, values of $H(e^-)$ and $H(H^+)$ are used, which are taken from literature (Marković et al., 2013a; Marković et al., 2016).

4.2 Influence of different free radicals on scavenging potency of various antioxidants

From a chemical point of view, free radicals are species containing one or more unpaired electrons. This particular characteristic is responsible for their high reactivity and triggering chain reaction mechanisms. Most of the radicals found in vivo are oxygen-centered free radicals (ROS) or reactive nitrogen species (RNS). The ROS are the superoxide anion radical ($O_2^{\bullet -}$), hydroxyl ($^{\bullet}OH$), alkoxyl ($RO^{\bullet}$), peroxyl ($ROO^{\bullet}$), and hydroperoxyl ($HOO^{\bullet}$) radicals. The RNS are peroxynitrite ($ONOO^-$), nitric oxide ($NO^{\bullet}$), and nitrogen dioxide ($NO_2^{\bullet}$). Among the oxygen-centered radicals, $^{\bullet}OH$ is the most electrophilic (Pryor, 1988) and reactive, with a half-life of $\sim 10^{-9}$ s. It can react through a wide variety of mechanisms, and its reactions with a large variety of chemical compounds take place at, or close to, diffusion-controlled rates (rate constants $\geq 10^9$ M/s). It has been estimated that $^{\bullet}OH$ is responsible for 60%–70% of tissue damage caused by ionizing radiation (Vijayalaxmi et al., 2004). A hydroxyl radical is so reactive that it is capable of immediate reacting, after formation, with almost any molecule in its vicinity and with little selectivity toward the various possible sites of attack. It has been held responsible for the most important oxidative damage to DNA (Chatgilialoglu et al., 2009). With respect to $^{\bullet}OH$, $ROO^{\bullet}$ radicals are less reactive species, capable of diffusing to remote cellular locations. Their half-lives are of the order of seconds (Pryor, 1986), and their electrophilicity is significantly lower than that of $^{\bullet}OH$ (Pryor, 1988). However, $ROO^{\bullet}$ can also react with other chemical species through different mechanisms. Peroxy radicals are, in general, less reactive than $HOO^{\bullet}$ when R is an alkyl or an alkenyl group (Galano, 2011). However, if R is a more efficient electron-accepting group, such as CCl_3, the reactivity of $ROO^{\bullet}$ toward organic molecules significantly increases (Milenković et al., 2017). Indeed, the rate constants for the electron-transfer reactions involving $ROO^{\bullet}$ strongly depend on the chemical nature of R. The rate constant significantly increases with the electron-

withdrawing character of the substituents (Neta et al., 1989). $RO^{\bullet}$ radicals are formed from the reduction of peroxides and are significantly more reactive than $ROO^{\bullet}$ radicals, provided that R is the same in both species, but they are less reactive than $^{\bullet}OH$ (León-Carmona et al., 2012).

On the other hand, RNS possess lower reactivity. The chemical reactivity of $NO^{\bullet}$ is rather limited, and as a consequence of that, its direct toxicity is less than that of ROS (Squadrito and Pryor, 1998). However, it reacts with $O_2^{\bullet-}$, yielding peroxynitrite (Radi et al., 2005), which is a very damaging species, as it is able to react with proteins, lipids, and DNA (Douki and Cadet, 1996). Nitrogen dioxide is a moderate oxidant, and its reactivity is somewhere between those of $NO^{\bullet}$ and $ONOO^{-}$ (Yan et al., 2014). It reacts with organic molecules at rates ranging from $\sim 10^4$ to 10^6 M/s, depending on the pH (Prütz et al., 1985).

The scavenging mechanisms are highly influenced by the electronic properties of the scavenged free radical species (Xie and Schaich, 2014). Bearing that in mind, the enthalpies of the reactants and products as well as of the reactions with described free radicals are calculated. It is well known that the values of the reaction enthalpies can significantly contribute to the understanding of the investigated reaction mechanisms. The reaction with the free radical ($RO^{\bullet}$) can occur via three mentioned mechanisms. In HAT/PCET mechanism, the reaction can be presented by Eq. (7.16):

$$A\text{–}OH + RO^{\bullet} \rightarrow A\text{–}O^{\bullet} + ROH \tag{7.16}$$

The SET-PT mechanism takes place in two steps, as it is described earlier in Eqs. (7.2) and (7.5). In interaction with free radicals ($RO^{\bullet}$), it can be presented by Eqs. (7.17) and (7.18):

$$A\text{–}OH + RO^{\bullet} \rightarrow A\text{–}OH^{\bullet+} + RO^{-} \tag{7.17}$$

$$A\text{–}OH^{\bullet+} + RO^{-} \rightarrow A\text{–}O^{\bullet} + ROH \tag{7.18}$$

The SPLET mechanism can be presented as follows:

$$A\text{–}OH + RO^{-} \rightarrow A\text{–}O^{-} + ROH \tag{7.19}$$

$$A\text{–}O^{-} + RO^{\bullet} \rightarrow A\text{–}O^{\bullet} + RO^{-} \tag{7.20}$$

The reaction of the examined compound with the particular free radical is considered thermodynamically favorable if it is exothermic:

$$\Delta_r H = \left[H(\text{products}) - H(\text{reactants})\right] < 0 \tag{7.21}$$

In radical inactivation, the HAT mechanism (Eq. 7.16) is characterized by the H-atom transfer from the examined compounds to the free radical ($RO^{\bullet}$). The value of $\Delta_r H_{BDE}$ can be calculated using the following equation:

$$\Delta_r H_{BDE} = \left[H(\text{A–O}^{\bullet}) + H(\text{ROH})\right] - \left[H(\text{A–OH}) + H\left(\text{RO}^{\bullet}\right)\right] \tag{7.22}$$

The SET-PT mechanism is described with Eqs. (7.17) and (7.18). The first step of this mechanism is determined by $\Delta_r H_{IP}$, while the second step is determined by $\Delta_r H_{PDE}$ (Eqs. 7.23 and 7.24, respectively):

$$\Delta_r H_{IP} = \left[H\left(\text{A–OH}^{\bullet+}\right) + H(\text{RO}^{-})\right] - \left[H(\text{A–OH}) + H\left(\text{RO}^{\bullet}\right)\right] \tag{7.23}$$

$$\Delta_r H_{PDE} = \left[H(\text{A–O}^{\bullet}) + H(\text{ROH})\right] - \left[H\left(\text{A–OH}^{\bullet+}\right) + H(\text{RO}^{-})\right] \tag{7.24}$$

$\Delta_r H_{PA}$ and $\Delta_r H_{ETE}$ are the reaction enthalpies related to the SPLET mechanism (Eqs. 7.19 and 7.20), and they are calculated using Eqs. (7.25) and (7.26), respectively:

$$\Delta_r H_{PA} = [H(\text{A–O}^{-}) + H(\text{ROH})] - [H(\text{A–OH}) + H(\text{RO}^{-})] \tag{7.25}$$

$$\Delta_r H_{ETE} = \left[H(\text{A–O}^{\bullet}) + H(\text{RO}^{-})\right] - \left[H(\text{A–O}^{-}) + H\left(\text{RO}^{\bullet}\right)\right] \tag{7.26}$$

5 MECHANISTIC APPROACH

In the case of the transition states, it was verified, by Intrinsic Coordinate Calculations (IRC), that the imaginary frequency corresponds to the expected motion along the reaction coordinate. These calculations

proved that each transition state (TS) connects two corresponding energy minima: reactant complex (RC) and product complex (PC). Natural bond orbital (NBO) analysis was performed for all participants in simulated reaction (Carpenter and Weinhold, 1988). Transition state theory (TST) affords one of the simplest theoretical approaches for estimating the rate constants (k), which requires only structural, energetic, and vibrational frequency information for reactants and transition states (Galano et al., 2014). The main advantage of using conventional TST is that it requires very limited potential energy information (only on reactants and the transition state), which makes it practical for a wide range of chemical reactions. Despite its relative simplicity, this theory has been proven to be sufficient to reproduce experimental rate constants of free radical-scavenging reactions (Galano and Alvarez-Idaboy, 2013). The rate constants were calculated using TST, implemented in TheRate program (Duncan et al., 1998), and 1 M standard state is calculated as follows:

$$k^{TST} = \frac{k_B T}{h} \exp\left(\frac{-\Delta G^{\neq}}{RT}\right) \tag{7.27}$$

where k_B and h stand for the Boltzman and Planck constants and $\Delta G^{\neq}$ is the free energy of activation, which is calculated as the difference in energies between transition states and reactants. Reaction path degeneracy ($ó$) and transmission coefficient$\gamma(T)$were taken into account, implying that the Eyring equation was transformed into the following:

$$k_{ZCT} = \sigma\gamma\,(T)\,\frac{k_B T}{h} \exp\left(\frac{-\Delta G^{\neq}}{RT}\right) \tag{7.28}$$

The transmission coefficient γ, corrections for tunneling effects (defined as the Boltzman average of the ratio between the quantum and classical probabilities), was calculated using the zero-curvature tunneling (ZCT) approach (Marcus, 1964).

5.1 Electron-transfer reaction rate constant calculation

One of the viable mechanisms to scavenge free radicals is electron transfer (ET), as the second step of the SPLET mechanism (Eq. 7.4) (Burton and Ingold, 1984).

Transition states are necessary for calculating the rate constant k_{TST}, Eq. (7.27), for HAT reactions. However, for electron-transfer reaction,

transition state cannot be located using electronic structure methods, as it is not possible to describe mechanistic pathway of electron motion. To estimate the reaction barrier (the term $\Delta G^{\neq}$) in such cases, the Marcus theory was used (Marcus, 1997). Within this transition-state formalism, the SPLET activation barrier ($\Delta G_{ET}^{\neq}$) is defined in terms of the free energy of reaction ($\Delta G_{ET}{}^{0}$) and the nuclear reorganization energy (λ):

$$\Delta G_{ET}^{\neq} = \frac{\lambda}{4}\left(1 + \frac{\Delta G_{ET}^{0}}{\lambda}\right)^{2} \tag{7.29}$$

λ is the energy associated with the nuclear rearrangement involved in the formation of products in an ET reaction, which implies not only the nuclei of the reacting species but also those of the surrounding solvent. For λ calculation, a very simple approximation was used:

$$\lambda \approx \Delta E_{ET} - \Delta G_{ET}^{0} \tag{7.30}$$

where ΔE is the nonadiabatic energy difference between reactants and vertical products, that is, A–O$^{\bullet}$ and RO^{-} in geometries of A–O^{-} and RO$^{\bullet}$:

$$\Delta E_{ET} = E(\mathrm{A-O^{\bullet}}) + E(\mathrm{RO^{-}}) - E(\mathrm{A-O^{-}}) - E\left(\mathrm{RO^{\bullet}}\right) \tag{7.31}$$

The adiabatic Gibbs free energies of reaction were calculated as follows:

$$\begin{aligned}\Delta G_{ET}^{0} = {} & G(\mathrm{A-O^{\bullet}}) + G(\mathrm{RO^{-}}) \\ & - G(\mathrm{A-O^{-}}) - G\left(\mathrm{RO^{\bullet}}\right)\end{aligned} \tag{7.32}$$

This approach is similar to that that was used by Nelsen and coworkers (Nelsen et al., 1987) for a large set of self-exchange reactions.

The theory of diffusion-controlled reaction was originally utilized by Alberty, Hammes, and Eigen to estimate the upper limit of enzyme-substrate reactions (Alberty and Hammes, 1958). According to their estimation, the upper limit of enzyme-substrate reactions was $10^{9}\ \mathrm{M^{-1}\,s^{-1}}$ (Eigen and Hammes, 2006). This fact has influence on the final value of steady-state Smoluchowski rate constant, k_D (Smoluchowski, 1918). If calculated rate constant is close to the diffusion limit, appropriate corrections are considered (the Collins-Kimball theory) as proposed by Galano and Alvarez-Idaboy (2013).

The apparent rate constant is then calculated as the correction to this value, according to the Collins-Kimball theory (Collins and Kimball, 1949):

$$k_{app} = \frac{k_D k_{TST}}{k_D + k_{TST}} \tag{7.33}$$

The steady-state Smoluchowski rate constant (k_D) (Smoluchowski, 1918), under the assumption of the irreversible bimolecular diffusion-controlled reaction, is calculated to encounter diffusion as a parameter. The diffusion-limited rate constant depends on the reactant distance, the diffusion coefficient of reactants, and Avogadro's constant:

$$k_D = 4\pi R D_{AB} N_A \tag{7.34}$$

where R denotes the reaction distance, N_A is the Avogadro number, and D_{AB} is the mutual diffusion coefficient of the reactants, A (anion of antioxidant A–O$^-$) and B free radical (RO$^\bullet$).

The Stokes-Einstein theory allows the calculation of the diffusion coefficient from Boltzmann's constant, temperature, viscosity of solvent, and radius of the solvent (Eq. 7.35) (Stokes, 1903). All of the reactions were investigated at 298 K:

$$D = \frac{k_B T}{6\pi\eta a} \tag{7.35}$$

The thermal rate constant (k) for hydroxyl radical is of the order of magnitude 10^9, and this value is at the upper limit of enzyme-substrate reaction, and because of that, one can say that reaction with hydroxyl radical is faster and diffusion controlled. When obtained rate constants are lower than 10^9, reaction is slower, and it is not controlled by diffusion.

6 THERMODYNAMICAL PARAMETERS FOR QUERCETIN, GALLIC ACID, AND DHBA

Antioxidative activity of phenolic compounds is usually examined by analyzing the thermodynamic properties of the parent molecules, the corresponding radicals, radical cations, and anions. Here, antioxidative properties were analyzed for different natural compounds, which are presented in Fig. 7.2. The generally accepted approach based on the

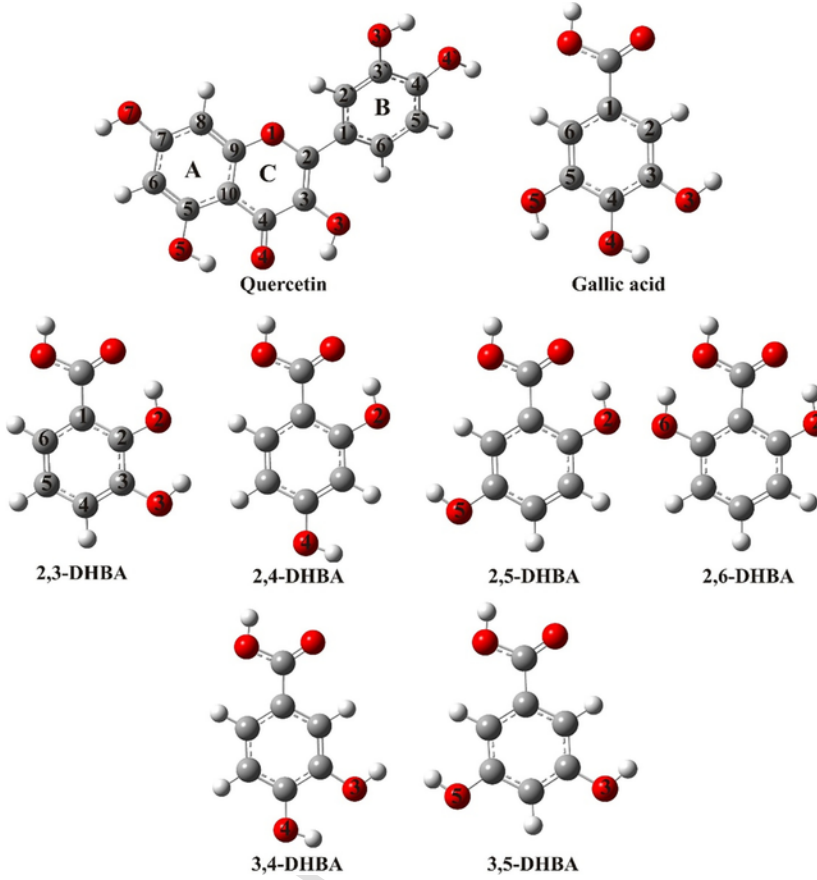

Fig. 7.2 The most stable structures of the investigated compounds.

thermodynamic parameters (BDE, IP, and PA), related to the HAT, SPLET, and SET-PT mechanisms, was applied. The calculations were performed in the gaseous phase (for Q), benzene and pentyl ethanoate (for GA, DHBAs) as nonpolar solvents, and in water (for these three considered compounds) and DMSO (for GA) as polar solvents. To estimate the effects of solvent, the SMD solvation model was used (Marenich et al., 2009). BDE, PA, and IP values provided insight into the thermodynamically most favorable reaction pathway. It was found that IP values are the highest for all investigated compounds, on the bases of the mutual comparison of the thermodynamical parameters, indicating that SET-PT mechanism is not the operative mechanism for all examined compounds, both in polar and nonpolar solvents. On the other hand, it

can be concluded that HAT and PCET are preferred antioxidative mechanisms in the gas phase for Q, due to the fact that the BDE values of Q are significantly lower than the corresponding IP and PA values (Marković et al., 2013b). Taking into account BDE and PA values for GA and DHBAs in benzene as a common nonpolar solvent, it is evident that BDE values are significantly lower than the corresponding PA values, which indicates that reaction in benzene probably proceeds via HAT mechanism. Also, the HAT mechanism is a predominant reaction pathway for some other natural compounds in benzene, such as baicalein (Marković et al., 2014a), morin (Marković et al., 2012b), and morin 2′-O^- phenoxide anion (Marković et al., 2012c). Regarding the obtained results for phenolic acids, it is evident that in polar solvent (water) and in nonpolar solvent (pentyl ethanoate), PA values are significantly lower than the corresponding BDE values for DHBAs and GA. These results unequivocally favor SPLET mechanism as the most probable reaction pathway. Further analysis of the thermodynamic parameters for DHBAs indicates that 3,4-DHBA and 2,3-DHBA have the best antioxidant activity in all solvents under investigation. The SPLET has been characterized as a crucial mechanism in the scavenging activity of numerous compounds in polar environments. Some examples are alizarin and alizarin red S (Jeremić et al., 2014), hydroxybenzoic and dihydroxybenzoic acids (Marković et al., 2014b; Milenković et al., 2017), kaempferol (Marković et al., 2014c), gallic acid (Đorović et al., 2014), erodiol (Marković et al., 2013c), baicalein (Marković et al., 2014a, b, c), and purpurin (Jeremić et al., 2012).

It should be pointed out that the influence of the polarity of the environment plays an important role in the feasibility of HAT and SPLET reaction mechanisms of investigated compounds. In addition to the polarity of the reaction medium, its acidity also plays an important role in antioxidative processes. In a polar protic solvent, such as aqueous solution, the environmental pH of the solution plays an important role in the changes of the reaction pathway of the antioxidant action. In acidic environment (when the pH is lower than the pK_a of the investigated compound), neutral form of the investigated molecule is predominant one. It should be expected that HAT or/and PCET are the main reaction pathways of an antioxidant action, for the investigated antioxidants, in this case. In the other case, when the pH is higher than the pK_a (basic environment), the anion species will prevail, indicating SPLET as the

main reaction pathway in this case. The first step of the SPLET mechanism is the formation of the corresponding anion that is strongly solvated in the aqueous medium. On the other hand, free radicals are not solvated in the same way as ions. It is crucial for a solvent to have an unpaired electron to solvate free radicals. However, the interactions between free radicals are weak, because the solvents have all their electrons paired. In this case, water (as a polar solvent) increases molecular mobility and rate of reaction, reducing radical lifetime. Obtained results for all analyzed compounds in water revealed that SPLET mechanism is a predominant reaction pathway. The stronger synergistic antioxidant activity should be expected at pH values close to 7. Then, it should be expected the reaction to take place via both reaction paths.

From presented results, it is clear that C4′–OH and C4–OH positions should be more reactive OH sites of Q and GA, respectively. These groups have the lowest BDE values in all phases, so they represent the most probable sites of H-atom abstraction (Marković et al., 2013b; Đorović et al., 2014). Also, PA values of all presented OH groups of Q and GA indicate that proton transfer from C4′–OH and C4–OH groups is easier compared with other OH groups, in all phases. On the other hand, the C3–OH position of 3,4- and 2,3-DHBAs is the most favorable site for homolytic O–H cleavage in all solvents. The obtained results for PA imply the proton transfer from C4–OH of 3,4-DHBA as favored, while the C3–OH group of 2,3-DHBA is preferably the site for heterolytic cleavage of the O–H bond, in all solvents.

7 ANTIRADICAL MECHANISMS IN THE PRESENCE OF DIFFERENT FREE RADICALS

The preferred mechanism of the antiradical activity of the considered compounds (Fig. 7.2) can be estimated from ΔH_{BDE}, ΔH_{IP}, and ΔH_{PA} values, namely, the lowest of these values indicates which mechanism is favorable.

The values of enthalpies of the reactions related to the HAT, SPLET, and SET-PT mechanisms of GA with three free radicals, $O_2^{\bullet -}$, $^{\bullet}OH$, and $CH_3OO^{\bullet}$ (methylperoxyl), imply 4-OH group as the most favorable site for homolytic and heterolytic O–H cleavage in all solvents (Đorović et al., 2014). The SET-PT mechanism is not a suitable pathway for the

reactions of GA with three examined radicals in all solvents. On the basis of the procedure based on the assessment of the reaction enthalpies of GA with selected radical species, it can be said that HAT mechanism is the preferable reaction pathway only for the reaction of GA with $^{\bullet}OH$ in water. Also, it should be pointed out that there is no mechanism suitable for the reaction of GA with $O_2^{\bullet -}$, in water. On the other hand, the SPLET mechanism is more favorable in nonpolar solvents, benzene and pentyl ethanoate. It should be emphasized that ΔH_{PA} value is lower by 46 kJ mol^{-1} than ΔH_{BDE}, when $CH_3OO^{\bullet}$ reacts with GA in the aqueous medium. The careful analysis of the results showed that change of the solvent polarity considerably influences the enthalpy of the investigated reactions. Namely, ΔH_{PA} values decrease when solvent polarity decreases, while ΔH_{BDE} values remain almost constant. All these facts indicate that SPLET is the prevailing mechanism in nonpolar solvents, while HAT is favorable one in polar solvents such as water. In addition, both of these mechanisms are competitive in DMSO.

The enthalpies for the reactions of $HO^{\bullet}$ with GA and Q show that these reactions in water solution are considerably more exothermic when it obeys HAT mechanism than when it takes place via SPLET mechanism (Table 7.1). Similarly, as in the case of GA, superoxide anion radical cannot be scavenged in reaction with Q, because all values for reaction enthalpies are positive, as can be seen in Table 7.1. On the other hand, exothermic reaction of Q with $^{\bullet}OH$ and $^{\bullet}OOCH_3$ implies inactivation of these two radicals via reactions of HAT and SPLET mechanisms. In the case of hydroxyl radical, low negative values of reaction enthalpies suggest HAT as more plausible antioxidative mechanism. The values of the enthalpies for reactions with the methylperoxyl radical indicate that SPLET is the most likely mechanism of an antioxidant action. Hydroxyl group in position C4′ is more reactive than others in both cases. This result is in agreement with results obtained by standard procedure. It is obvious that all three investigated radicals react by the same mechanisms with both Q and GA, in aqueous environment.

The following text presents the results obtained for the inactivation of the previously mentioned free radicals with DHBAs in solvents of different polarity. From Tables 7.2–7.4 it can be noted that DHBAs can inactivate all examined free radicals. The polarity of solvent plays an important role in determining the mechanism of antioxidant action.

Table 7.1 Calculated reaction enthalpies (kJ mol^{-1}), for the reactions of Q and GA with hydroxyl radical, superoxide radical anion, and peroxyl radical in water.

	Water ε = 78.35				
Water ε = 78.35	***HAT***	***SET-PT***		***SPLET***	
	ΔH_{BDE}	ΔH_{IP}	ΔH_{PDE}	ΔH_{PA}	ΔH_{ETE}
		29			
Q-OH–3 +•OH	− 158		− 187	− 72	− 86
Q-OH–3′+•OH	− 147		− 176	− 78	− 69
Q-OH–4′+•OH	− 154		− 183	− 87	− 67
GA-OH-4 +•OH	− 159	57	− 216	− 101	− 58
		282			
Q-OH–3 +•OO^-	48		− 234	40	7
Q-OH–3′+•OO^-	58		− 223	35	24
Q-OH–4′+•OO^-	51		− 231	26	26
GA-OH–4 +•OO^-	48	311	− 263	9	39
		127			
Q-OH–3 +•$OOCH_3$	− 21		− 148	− 34	13
Q-OH–3′+•$OOCH_3$	− 10		− 137	− 40	30
Q-OH–4′+•$OOCH_3$	− 17		− 144	− 49	31
GA-OH–4 +•$OOCH_3^-$	− 18	160	− 178	− 64	46

Unlike GA and Q, DHBAs will react with superoxide anion radical in nonpolar solvent benzene via SPLET mechanism (Table 7.3).

Regarding hydroxyl and methylperoxyl radicals, both can be inactivated via HAT or SPLET mechanism depending on the solvent polarity (Table 7.2). In the case of inactivation of hydroxyl radical, there is a competition between HAT and SPLET. The HAT is prevalent mechanism in water, while SPLET is a predominant scavenging mechanism in benzene. As for the deactivation of methylperoxyl radical, it was found that SPLET is dominant antiradical mechanism in both solvents for all examined DHBAs (Table 7.4).

Table 7.2 Calculated reaction free energy (kJ mol^{-1}) for the reactions of DHBAs with hydroxyl radical.

	Water ε = 78.35					**Benzene ε = 2.27**				
DHBAs	***HAT***	***SET-PT***		***SPLET***		***HAT***	***SET-PT***		***SPLET***	
	ΔH_{BDE}	ΔH_{IP}	ΔH_{PDE}	ΔH_{PA}	ΔH_{ETE}	ΔH_{BDE}	ΔH_{IP}	ΔH_{PDE}	ΔH_{PA}	ΔH_{ETE}
2.3-DHBA		93					360			
2-OH	− 127		− 220	− 4	− 123	− 113		− 473	− 170	57
3-OH	− 138		− 231	7	− 136	− 124		− 484	− 159	42
2.4-DHBA		75					389			
2-OH	− 97		− 171	− 64	− 33	− 70		− 460	− 140	70
4-OH	− 104		− 179	− 81	− 23	− 99		− 488	− 191	93
2.5-DHBA		29					345			
2-OH	− 132		− 161	− 57	− 75	− 101		− 446	− 131	30
5-OH	− 146		− 176	− 57	− 89	− 140		− 485	− 148	8
2.6-DHBA		46					361			
2-OH	− 114		− 159	− 61	− 52	− 87		− 448	− 145	57
6-OH	− 125		− 171	− 73	− 52	− 109		− 470	− 169	60
3.4-DHBA		57					379			
3-OH	− 144		− 201	− 80	− 64	− 144		− 524	− 192	47
4-OH	− 141		− 198	− 91	− 50	− 143		− 522	− 210	67

Table 7.2 (Continued)

	Water ε = 78.35					**Benzene ε = 2.27**				
DHBAs	***HAT***	***SET-PT***		***SPLET***		***HAT***	***SET-PT***		***SPLET***	
	ΔH_{BDE}	ΔH_{IP}	ΔH_{PDE}	ΔH_{PA}	ΔH_{ETE}	ΔH_{BDE}	ΔH_{IP}	ΔH_{PDE}	ΔH_{PA}	ΔH_{ETE}
3.5-DHBA		62					384			
3-OH	− 122		− 183	− 66	− 56	− 115		− 499	− 164	49
5-OH	− 122		− 184	− 67	− 56	− 116		− 500	− 165	49

Table 7.3 Calculated reaction free energy (kJ mol^{-1}) for the reactions of DHBAs with superoxide anion radical.

	Water ε = 78.35					**Benzene ε = 2.27**				
DHBAs	***HAT***	***SET-PT***		***SPLET***		***HAT***	***SET-PT***		***SPLET***	
	ΔH_{BDE}	ΔH_{IP}	ΔH_{PDE}	ΔH_{PA}	ΔH_{ETE}	ΔH_{BDE}	ΔH_{IP}	ΔH_{PDE}	ΔH_{PA}	ΔH_{ETE}
2.3-DHBA		348					938			
2-OH	81		− 267	106	− 26	121		− 817	− 15	136
3-OH	70		− 278	117	− 39	110		− 828	− 4	122
2.4-DHBA		329					968			
2-OH	111		− 219	47	64	164		− 804	14	150
4-OH	103		− 226	29	74	135		− 833	− 37	172
2.5-DHBA		284					426			
2-OH	76		− 208	53	22	41		− 384	− 69	111
5-OH	61		− 223	53	8	3		− 423	− 86	89
2.6-DHBA		300					939			
2-OH	94		− 207	49	45	147		− 792	10	137
6-OH	82		− 218	37	45	125		− 814	− 15	140
3.4-DHBA		312					958			
3-OH	64		− 248	31	33	90		− 868	− 37	127
4-OH	66		− 245	19	47	91		− 867	− 55	146

Table 7.3 (Continued)

	Water $\varepsilon = 78.35$					Benzene $\varepsilon = 2.27$				
DHBAs	***HAT***	***SET-PT***		***SPLET***		***HAT***	***SET-PT***		***SPLET***	
	ΔH_{BDE}	ΔH_{IP}	ΔH_{PDE}	ΔH_{PA}	ΔH_{ETE}	ΔH_{BDE}	ΔH_{IP}	ΔH_{PDE}	ΔH_{PA}	ΔH_{ETE}
3.5-DHBA		316					963			
3-OH	85		− 231	44	41	119		− 844	− 9	128
5-OH	85		− 231	43	42	118		− 845	− 11	129

Table 7.4 Calculated reaction free energy (kJ mol^{-1}) for the reactions of DHBAs with methylperoxyl radical.

	Water ε = 78.35					**Benzene ε = 2.27**				
DHBAs	***HAT***	***SET-PT***		***SPLET***		***HAT***	***SET-PT***		***SPLET***	
	ΔH_{BDE}	ΔH_{IP}	ΔH_{PDE}	ΔH_{PA}	ΔH_{ETE}	ΔH_{BDE}	ΔH_{IP}	ΔH_{PDE}	ΔH_{PA}	ΔH_{ETE}
2.3-DHBA		197					441			
2-OH	14		− 183	33	− 19	30		− 411	− 108	138
3-OH	3		− 194	44	− 33	19		− 422	− 97	123
2.4-DHBA		178					470			
2-OH	44		− 134	− 26	71	73		− 398	− 78	151
4-OH	37		− 142	− 44	81	44		− 426	− 130	174
2.5-DHBA		133					426			
2-OH	9		− 124	− 20	29	41		− 384	− 69	111
5-OH	− 6		− 138	− 20	14	3		− 423	− 86	89
2.6-DHBA		149					442			
2-OH	27		− 122	− 24	51	56		− 386	− 83	138
6-OH	16		− 133	− 36	52	34		− 408	− 107	141
3.4-DHBA		161					460			
3-OH	− 3		− 164	− 42	40	− 2		− 462	− 130	128
4-OH	0		− 161	− 54	54	0		− 460	− 148	148

Table 7.4 (Continued)

	Water ε = 78.35					**Benzene ε = 2.27**				
DHBAs	***HAT***	***SET-PT***		***SPLET***		***HAT***	***SET-PT***		***SPLET***	
	ΔH_{BDE}	ΔH_{IP}	ΔH_{PDE}	ΔH_{PA}	ΔH_{ETE}	ΔH_{BDE}	ΔH_{IP}	ΔH_{PDE}	ΔH_{PA}	ΔH_{ETE}
3.5-DHBA		165					465			
3-OH	19		− 146	− 29	48	28		− 437	− 102	130
5-OH	18		− 147	− 30	48	27		− 438	− 103	130

8 MECHANISTIC APPROACH TO ANALYSIS OF THE ANTIOXIDANT ACTION

8.1 Reaction of quercetin via HAT mechanism

Bearing in mind the predicted reactivity of OH groups of Q, obtained on the basis of the BDE values (Marković et al., 2010), the potential antioxidant activity of Q is studied with the simulation of the reaction with hydroperoxyl radical, Q + •OOH → Q• + HOOH (Scheme 7.1).

The analysis of the NBO charges and orbital occupancies (Tables 7.5 and 7.6) as well as the SOMOs of the reactants, transition states, and products (Fig. 7.3) showed that the reaction of Q with the hydroperoxyl radical is governed by HAT mechanism (Marković et al., 2010; Dhaouadi et al., 2009). Namely, the analysis of NBO charges of TSs shows that the QO and HOO fragments have negative charge, while transferred H has a positive charge (amount 0.5) in all cases (Table 7.5). The spin density is also located on QO and HOO fragments. In comparison with the RC, the spin density on QO moiety increased, while spin density related with OOH fragment decreased. However, the spin density on the transferred hydrogen atom is equal to zero. These facts indicate that reactions of OH groups of quercetin with •OOH radical proceed via HAT mechanism.

From Table 7.6, it can be seen that an unpaired electron is located in *p*-orbital on the Op1 oxygen atom in •OOH radical (Scheme 7.2). There is overlapping between *p*-orbital and *s*-orbital of Hn atom from OH group of Q leading to a formation of the H-Op1 bond (occupancy is close to 1.7). In addition, after cleavage of On–Hn (index n represents to the number of positions of OH groups) bond, the unpaired electron stays in the *p*-orbital of On leading to the overlapping between the *p*-orbitals of On and Cn and formation of the *p*-bonds with relatively high occupancies (about 1.7). In each TSn, the unpaired electron is mainly located in antibonding orbitals (BD(2)*CnOn) and (BD(1)*HnOp1) that are relatively highly occupied.

The SOMO of TSs (Fig. 7.3) shows that unpaired electron is mainly delocalized among ring B, C3 atom of the ring C, and corresponding oxygen atoms that are deprotonated. In addition, the delocalization of SOMOs is significantly weaker in TS5 and TS7 than in other three TSs. These differences can be explained in the higher activation energies for the reactions in position 5 and 7.

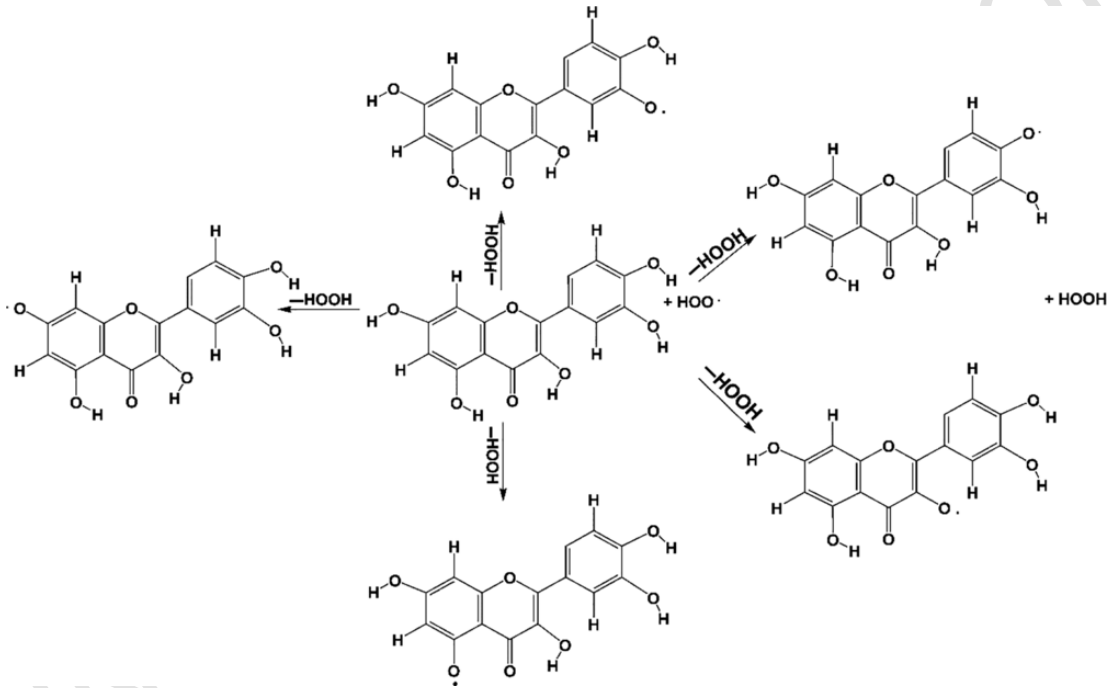

Scheme 7.1 The five reaction pathways for reaction of quercetin with hydroperoxyl radical.

Table 7.5 Some NBO charges and spin densities for the reactants, transition states, and products.

Reactants			**TS**			**Products**		
	Nat. charg.	***Spin dens.***		***Nat. charg.***	***Spin dens.***		***Nat. char.***	***Spin dens.***
QO4′H4′	0	0.00	QO4′	− 0.28	0.46	QO4′	0	1
			H4′	0.52	− 0.03			
OOH	0	1.00	OOH	− 0.24	0.57	HOOH	0	0
			QO3′	− 0.27	0.47	QO3′	0	1
			H3′	0.52	− 0.03			
			OOH	− 0.25	0.56	HOOH	0	0
			QO3	− 0.17	0.49	QO3	0	1
			H3	0.52	− 0.03			
			OOH	− 0.35	0.54	HOOH	0	0
			QO5	− 0.27	0.56	QO5	0	1
			H5	0.53	− 0.02			
			OOH	− 0.26	0.46	HOOH	0	0
			QO7	− 0.25	0.54	QO7	0	1
			H7	0.52	− 0.03			
			OOH	− 0.27	0.49	HOOH	0	0

Table 7.6 Some selected NBO orbital occupancies and orbital energies.

NBO	Quercetin		Transition		Products	
	Occ.	*Ener*	*Occ.*	*Ener*	*Occ.*	*Ener*
BD1 C4′O4′	1.99		1.99	− 1.074	1.99	− 1.171
BD2 C4′O4′			1.74	− 0.531	1.92	− 0.479
BD1* C4′O4′			0.03	0.471	0.01	0.622
BD2* C4′O4′			0.79	− 0.095	0.35	− 0.010
BD H4′O4′	1.99	− 0.879				
BD H4′O1			1.70	− 0.570		
BD *H4′O1			0.29	0.259		
BD1 C3′O3′			1.99	− 1.090	1.99	− 1.160
BD2 C3′O3′			1.76	− 0.494	1.90	− 0.481
BD1* C3′O3′			0.01	0.506	0.01	0.607
BD2 *C3′O3′			0.70	− 0.073	0.40	− 0.026
BD H3′O3′	1.99	− 0.853				
BD H3′O1			1.76	− 0.640		
BD *H3′O1			0.23	0.335		
BD1 C3O3			1.99	− 1.090	1.99	− 1.174
BD2 C3O3			1.78	− 0.508	1.91	− 0.479
BD1* C3O3			0.01	0.503	0.01	0.634
BD2* C3O3			0.78	− 0.091	0.35	− 0.016
BD H3O3	1.99	− 0.850				
BDH3O1			1.73	− 0.601		
BD*H3O1			0.27	0.301		
BD1 C5O5	1.99	− 1.048	1.99	− 1.120	1.99	− 1.175
BD2 C5O5			1.82	− 0.484	1.89	− 0.471
BD1* C5O5			0.01	0.546	0.01	0.638
BD2* C5O5			0.54	− 0.029	0.27	0.015
BD H5O5	1.99	− 0.860				
BD H5O1			1.83	− 0.712		
BD* H5O1			0.19	0.403		
BD1 C7O7	2	− 1.053	1.99	− 1.093	2	− 1.160
BD2 C7O7			1.75	− 0.498	1.84	− 0.474
BD1* C7O7			0.02	0.503	0.01	0.616
BD2* C7O7			0.63	− 0.057	0.32	− 0.004

Table 7.6 (Continued)

NBO	Quercetin		Transition		Products	
	Occ.	*Ener*	*Occ.*	*Ener*	*Occ.*	*Ener*
BD H7O7	1.99	− 0.868				
BD H7O1			1.77	− 0.640		
BD* H7O1			0.23			
HOO radical						
BD1 OO1	2	− 1.049				
BD2 OO1						
Lp1 O	2	− 0.836				
Lp2 O	1.74	− 0.508				
Lp3 O						
Lp1 O1	2	− 0.836				
Lp2 O1	1.98	− 0.515				
Lp3 O1	1.25	− 0.496				
BD OH	2	− 0.904				

The most reactive sites are 3′–OH and 4′–OH. The reaction in the 3′–OH position is faster than one in the 4′–OH position. This result is slightly different from the BDE results, since the 4′–OH radical form has lower BDE value. It means that the reaction with the $^{\bullet}$OH radical is kinetically controlled. Also, the differences between HAT and PCET mechanisms, examining geometry orientations of peroxyl radical toward Q in transition states (Fig. 7.3), were considered. It was found that PCET is energetically unfavorable (e.g., for Q3′ and Q4′, the activation energies are higher by 3.6 and 2.6 kcal mol^{-1}) compared with HAT. These results are in good agreement with the results obtained by the examination of the reactions of flavonoids with peroxyl and DPPH radicals in nonpolar solvent (Marković et al., 2010; Musialik et al., 2009).

8.2 Reaction of quercetin via SET-PT mechanism

The reaction $Q^{\bullet+} + R^- \rightarrow Q^{\bullet} + RH$ (Scheme 7.3) plays a significant role in determining which mechanism of Q is dominant. The thermodynamic parameter that characterizes this mechanism is PDE. For this purpose, reactions of the radical cation of quercetin ($Q^{\bullet+}$) with different anions (OH^-, CH_3S^-, and CH_3NH_2) were examined in gas and water.

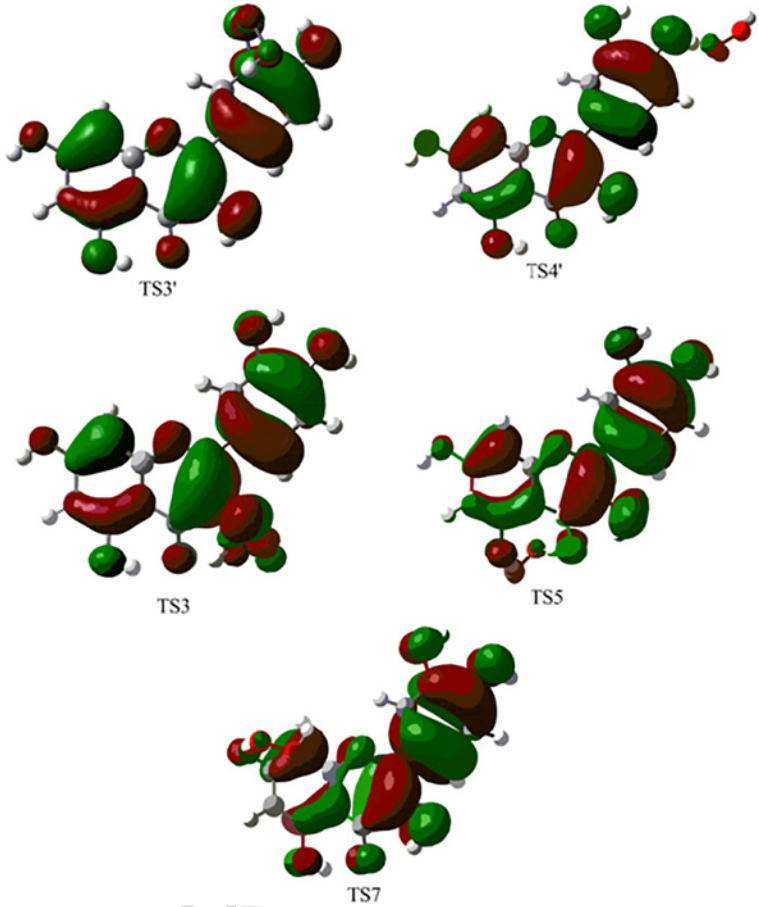

Fig. 7.3 The shapes of SOMOs in different transition states.

8.2.1 Mechanism $Q^{\bullet+}$ with the hydroxide anion in the gaseous and aqueous phases

The reaction with OH^- in gas phase (Scheme 7.3) takes place via the HAT mechanism (transition state is found), while the SET-PT mechanism is dominant in the aqueous phase (reaction is occurring without TS, Fig. 7.4). The finding that in some cases $Q^{\bullet+}$ undergoes HAT mechanism was quite unexpected. Namely, the hydroxide anion has two very high lying *p*-orbitals where the lone pairs are placed. Their energy (− 0.02274 au) is higher than that of the SOMO of $Q^{\bullet+}$ (− 0.41278 au). Thus, one of the HO^- electrons is spontaneously transferred to $Q^{\bullet+}$, yielding Q and

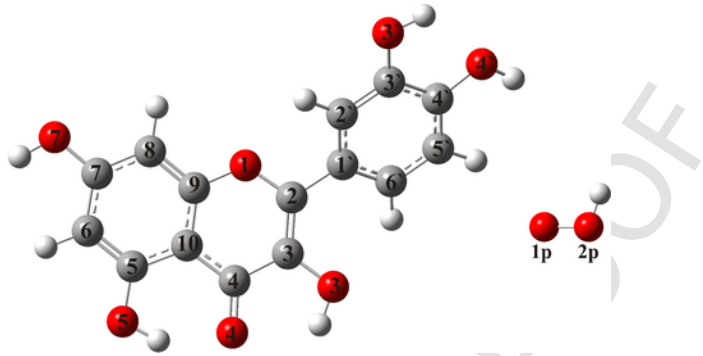

Scheme 7.2 Atomic numbering of quercetin and hydroperoxyl radical.

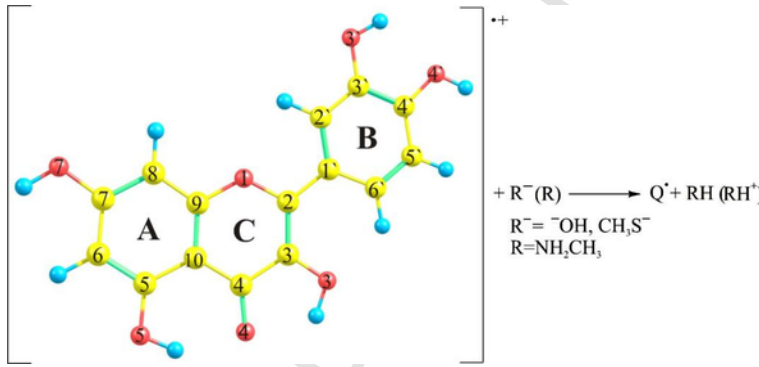

Scheme 7.3 General scheme of the investigated reactions.

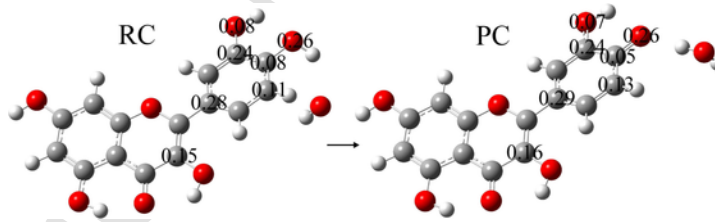

Fig. 7.4 Reaction in the position 4′ of $Q^{\bullet+}$ in the aqueous solution.

hydroxyl radical, which further reacts according to the HAT mechanism (gas phase). On the other hand, in water, a spontaneous electron transfer from the weak base to $Q^{\bullet+}$ does not occur (due to stronger attractions between the nuclei and lone pairs of the base), because the energy of the HOMOs of the hydroxide anion (− 0.31160 au) is lower than of SOMO

of $Q^{\bullet+}$ is (− 0.29050 au). For this reason, a spontaneous proton transfer from $Q^{\bullet+}$ to the base occurs (SET-PT) (Fig. 7.4). The reactions of $Q^{\bullet+}$ with the hydroxide anion via SET-PT in water proceed without reaction barrier, which require the reaction energy amount − 63.2, − 67.8, − 98.4, − 114.7, and − 121.1 kJ mol^{-1} for transformation of RCs to the corresponding PCs.

The thermodynamic and kinetic parameters for HAT reactions, in gas phase, are calculated. These parameters are collected in Table 7.7. The presented results show that the 4′–OH position is reactive site. The optimized geometries of RC, TS, and PC, for the most favorable reaction pathway (HAT), are depicted in Fig. 7.5

The obtained results emphasize the tunneling effect as responsible for accelerating the reaction between Q and hydroxyl radical. These indicate that the reaction of hydrogen atom abstraction involves the motion of

Table 7.7 The calculated values of kinetic parameters, in gas phase, for the reaction of $Q^{\bullet+}$ and HO^{-}.

Site	$\Delta G^{\neq}$ (kJ mol^{-1})	k^{TST} (s^{-1})	k^{ZCT} (s^{-1})	ΔG_r (kJ mol^{-1})
7	24.5	2.88×10^{8}	7.40×10^{9}	− 98.7
3′	23.2	6.01×10^{8}	5.93×10^{9}	− 128.6
3	23.1	7.46×10^{8}	3.69×10^{10}	− 130.7
4′	13.0	4.22×10^{10}	2.28×10^{11}	− 163.4

$\Delta G^{\neq}$, k^{TST}, k^{ZCT}, and ΔG_r denote activation free energy and rate constants and reaction free energy, respectively.

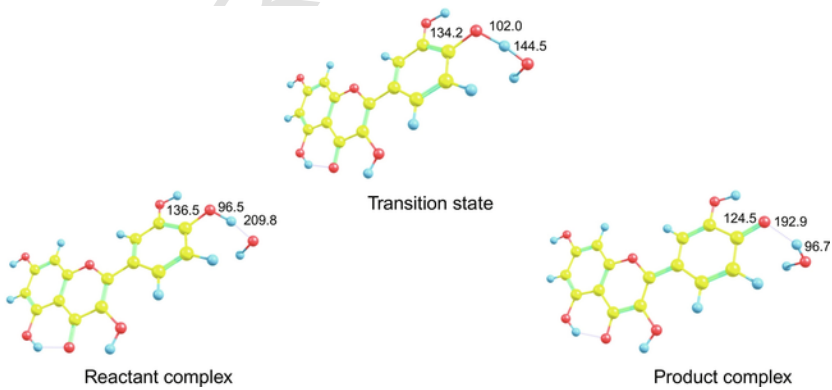

Fig. 7.5 The optimized geometries of the RC, TS, and PC for the most favorable hydrogen atom transfer reaction in position 4′–OH, with selected bond distances (pm).

hydrogen atom that can easily tunnel through the reaction barrier (reaction of HAT mechanism). This effect is responsible for increasing the reaction rate constant (k^{ZCT}) in all positions (Table 7.7). It is observed that this effect decreases with the increase of the temperature (Fig. 7.6). In addition, the reactions at the 4′ position of Q are extremely exothermic (Table 7.7). The obtained values of activation energies are low and corresponding rate constants are high. The homolytic bond cleavage between O4′ and H4′ atoms requires the lowest activation energy (and shows the highest rate constant values). The bond breaking at position 4′ is favorable due to the involvement of O4′ in a relatively strong hydrogen bond with H3′, leading to the weakness of the O4′–H4′ bond.

8.2.2 Mechanism $Q^{\bullet+}$ with the MeS anion

The energies of the HOMOs of the MeS anion in the gaseous and aqueous phases are amounts − 0.03088 and − 0.21923 au, that is, they are higher than the corresponding energies of the SOMOs of $Q^{\bullet+}$ (− 0.41278 and − 0.29050 au). The reaction $Q^{\bullet+} + CH_3S^- \rightarrow Q + CH_3S^\bullet$ (Fig. 7.7) is

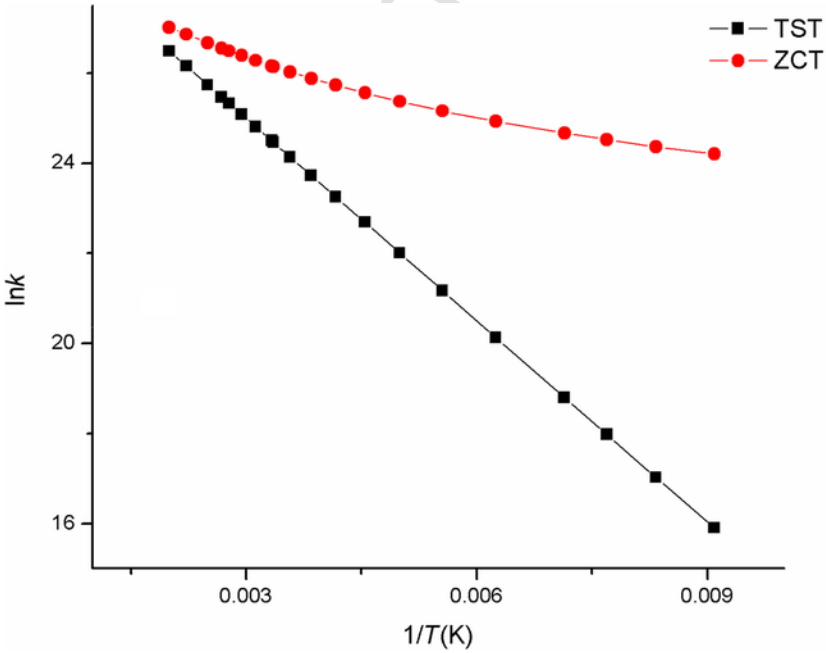

Fig. 7.6 Dependence of $\ln k^{TST}$ and $\ln k^{ZCT}$ on reciprocal temperature in the HAT pathways of $Q^{\bullet+}$ and hydroxide anion in position 4, in gas phase.

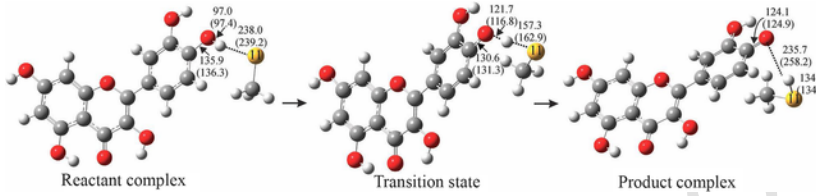

Fig. 7.7 Reaction path for the H-atom transfer from the 4′ position of Q to the $CH_3S^{\bullet}$ radical, with selected bond distances (pm). The values for bond distances in the aqueous solution are given in the brackets.

exothermic in both phases (ΔG_r =−562.2 and − 146.6 kJ mol^{-1}). For these reasons, an electron from a lone pair of the MeS anion spontaneously transfers to $Q^{\bullet+}$, yielding to Q and $CH_3S^{\bullet}$, which further proceed via the HAT mechanism.

The reactions of Q and $CH_3S^{\bullet}$, in position 4′, proceed via the TSs that require the free activation energies of 44.2 kJ mol^{-1} (gas) and 61.0 kJ mol^{-1} (water). Corresponding reaction paths are shown in the Fig. 7.7.

8.2.3 Mechanism $Q^{\bullet+}$ with the methylamine

The reaction of $Q^{\bullet+}$ with methylamine (CH_3NH_2) takes place via SET-PT mechanism, both in gaseous and aqueous media. It should be pointed out that in this case, TSs were not located, because these reactions are taking place without reaction barriers. Namely, the HOMO energy of CH_3NH_2 in the aqueous phase is amount − 0.31322 au, that is, it is lower than the corresponding energy of the SOMO of $Q^{\bullet+}$. On the other hand, HOMO energy of CH_3NH_2 (− 0.30685 au) is higher than the SOMO energy of $Q^{\bullet+}$ in the gas phase. The hypothetic reaction $Q^{\bullet+} + CH_3NH_2 \rightarrow Q + {}^{\bullet}CH_3NH_2$ is endothermic (ΔG_r = 132.4 kJ mol^{-1}). The energetics of this reaction is a consequence of the pronounced instability of the methylamine radical cation in comparison with the neutral parent molecule. On the basis of these facts, it can be supposed that an electron from a lone pair of methylamine will not spontaneously transfer to $Q^{\bullet+}$ and that Q can undergo the SET-PT mechanism, in both gaseous and aqueous phases.

The results for the reaction of $Q^{\bullet+}$ with methylamine in the gaseous and aqueous phases (Fig. 7.8) are mutually very similar. The reaction of the spontaneous transfer of phenolic hydrogen to N11 takes place without an activation barrier, followed by a system stabilization of − 72.6 kJ/mol

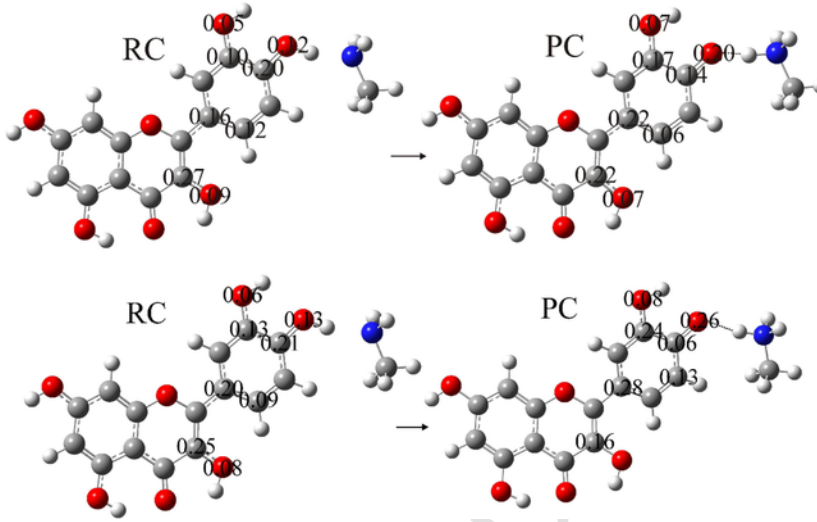

Fig. 7.8 Reaction in the 4′ position of $Q^{\bullet+}$ in the gaseous (*top*) and aqueous phase (*bottom*).

(gas phase) and − 77.6 kJ/mol (aqueous solution). Once spontaneously formed, $Q^{\bullet+}$ donates proton to methylamine in both phases, with system stabilization. These findings show that SET-PT is an acceptable mechanism of Q with methylamine.

9 KINETICS OF HAT AND PCET MECHANISM

The examination of differences between HAT and PCET mechanisms, including different positions of the reacting species and different electronic characters (Inagaki and Yamamoto, 2014), is one of the useful methods. By examining orientations of alkyl peroxyl radicals toward GA in transition states, the differences between HAT and PCET could be considered. The optimized structures of stationary points along reaction pathways of HAT mechanism in water and PCET mechanism in benzene with methylperoxyl radical are presented in Fig. 7.9.

The calculated values of kinetic parameters for the reaction of GA and free peroxy radicals are presented in Table 7.8. The obtained results show that the barriers are systematically higher in benzene than in polar media. Comparison of the reactivity of GA in positions 3 and 4 in both solvents shows that the energy barrier is significantly lower for the transfer of the H atoms of the 4-OH group. It should be pointed out that

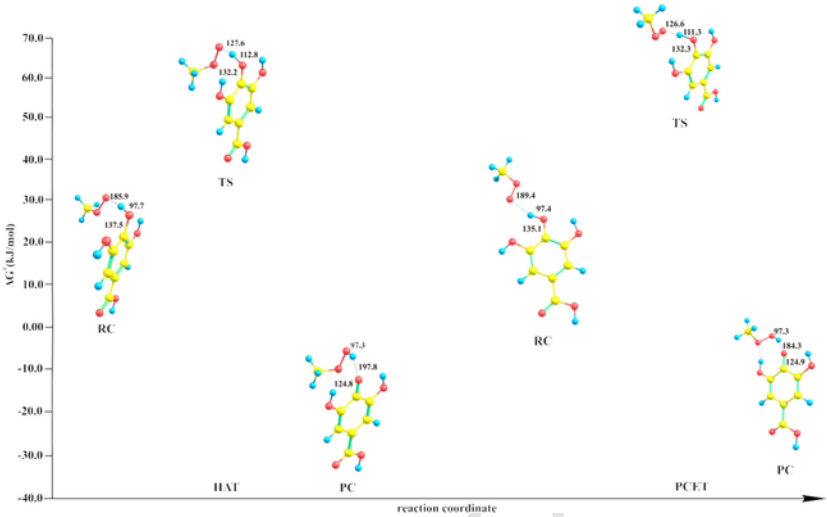

Fig. 7.9 Reaction pathway for the H-atom transfer from the C4–OH position of GA to the $CH_3OO^{\bullet}$ radical, in water and benzene. The distances between C = O, O–H, and H–O9 bonds are given in pm.

there is difference of about 20 kJ mol^{-1} in the case of HAT and about 10 kJ mol^{-1} for PCET. The obtained values of kinetic parameters are given in Table 7.8 (Milenković et al., 2017). The obtained values for activation energies and k^{TST} in water and benzene (Table 7.8) are in good accordance with thermodynamic results. On the basis of obtained values for ΔG_{BDE} and for the k^{TST} rate constants, it is clear that HAT is a predominant mechanism in both solvents. Moreover, PCET mechanism is not possible in water for investigated reaction. In addition, as a consequence of the barrier sharpening, a large tunneling effect is observed for both mechanisms (Table 7.8).

The highest rate constant values can be attributed to the involvement of O4 in the relatively strong hydrogen bonds within H3 and H5, contributing to the weakening of the O4–H4 bond. The obtained results, for thermodynamic and kinetic parameters, show that the reaction of methylperoxyl radical is preferred. The values of the rate constant in benzene, for PCET mechanism, indicated that position 4 is also more probable reactivity site (Table 7.8). However, the HAT mechanism is more probable mechanism than PCET, if comparing the obtained parameters for both mechanisms (Milenković et al., 2017).

Table 7.8 The calculated values of kinetic parameters for the reaction of GA and peroxy radicals.

	HAT			PCET		
	$\Delta G^{\neq}$ (kJ mol^{-1})	k^{TST} (M^{-1} s^{-1})	k^{ZCT} (M^{-1} s^{-1})	$\Delta G^{\neq}$ (kJ mol^{-1})	k^{TST} (M^{-1} s^{-1})	k^{ZCT} (M^{-1} s^{-1})
GA–3O$^{\bullet}$			Water			
MP	54.4	1.83×10^{3}	2.32×10^{6}	/	/	/
EP	63.3	5.01×10^{1}	1.05×10^{5}	/	/	/
iPP	65.8	1.86×10^{1}	4.07×10^{5}	/	/	/
tBP	69.3	4.00×10^{0}	9.28×10^{5}	/	/	/
GA–4O$^{\bullet}$						
MP	33.4	8.59×10^{6}	8.54×10^{8}	/	/	/
EP	34.0	6.82×10^{6}	8.19×10^{8}	/	/	/
iPP	36.9	2.16×10^{6}	6.49×10^{8}	/	/	/
tBP	39.8	6.51×10^{5}	1.23×10^{9}	/	/	/
GA–3O$^{\bullet}$			Benzene			
MP	59.9	1.97×10^{2}	1.15×10^{5}	73.1	9.75×10^{-1}	1.69×10^{4}
EP	61.2	1.16×10^{2}	8.29×10^{4}	74.7	5.00×10^{-1}	7.17×10^{4}
iPP	62.3	7.63×10^{1}	5.94×10^{4}	75.8	3.28×10^{-1}	2.09×10^{4}
tBP	62.7	6.37×10^{1}	1.31×10^{5}	76.0	3.06×10^{-1}	1.33×10^{4}
GA–4O$^{\bullet}$						

Table 7.8 (Continued)

	HAT			PCET		
	$\Delta G^{\neq}$ (kJ mol^{-1})	k^{TST} (M^{-1} s^{-1})	k^{ZCT} (M^{-1} s^{-1})	$\Delta G^{\neq}$ (kJ mol^{-1})	k^{TST} (M^{-1} s^{-1})	k^{ZCT} (M^{-1} s^{-1})
MP	39.7	6.79×10^5	5.17×10^7	63.9	3.99×10^1	2.20×10^6
EP	40.7	4.59×10^5	4.71×10^7	64.4	2.36×10^1	1.83×10^6
iPP	40.6	4.70×10^5	6.33×10^7	65.8	1.82×10^1	1.16×10^6
tBP	41.3	3.59×10^5	1.84×10^8	65.6	2.02×10^1	2.02×10^6

$\Delta G^{\neq}$, k^{TST}, and k^{ZCT} denote activation free energy and rate constants, respectively.

Additionally, to explain the differences between HAT and PCET mechanisms, the shapes of SOMOs of TSs are analyzed (Fig. 7.10). The obtained results show that SOMOs are not localized over O4 ⋯ H4 ⋯ O9 transition vector in TSs for PCET, while the HAT mechanism is characterized by a significant SOMO density along the donor ⋯ H ⋯ acceptor transition vector. In addition, the obtained values for HAT activation barriers are more favorable than the values for the PCET mechanism in all cases (about 24 kJ mol^{-1}). This unambiguously indicates HAT as the preferred mechanistic path under the investigated reaction conditions.

10 RADICAL ADDUCT FORMATION (RAF) MECHANISM

Marino and coworkers used DFT approach to examine the reaction of GA and its monoanion with •OH and •OOH radicals via RAF mechanism in water and benzene, as solvents (Marino et al., 2014). Comparison of the reactivity toward •OH and •OOH indicate that investigated compounds possess the higher reactivity toward •OH. It was found that

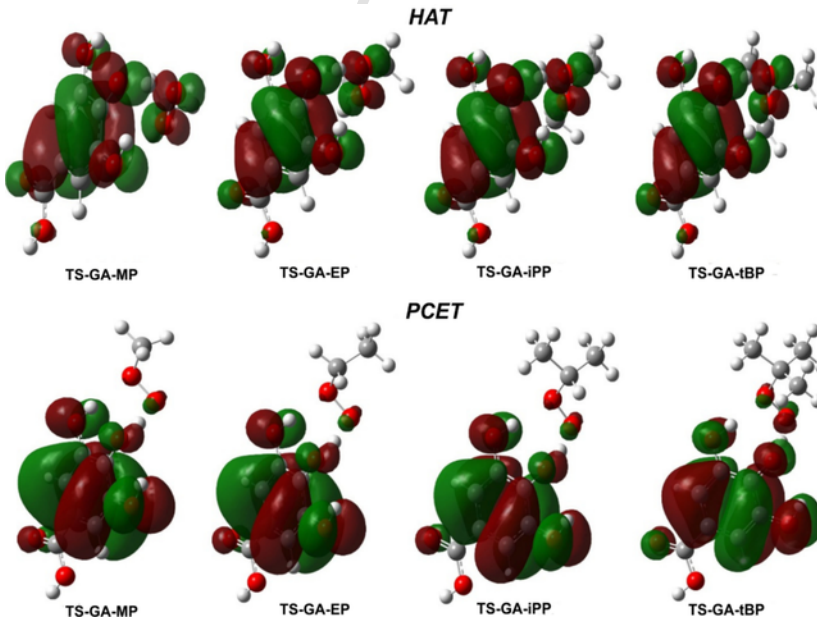

Fig. 7.10 The shape of SOMOs in different transition states of HAT and PCET mechanisms in position 4, in benzene.

the reactions that involve •OH are exergonic, while the reactions with •OOH are thermodynamically unfavorable (endogenic). Based on these facts, the exergonic reactions are selected for further mechanistic investigation.

To calculate the rate constants for RAF mechanistic pathway with hydroxyl radical, transition states were found in water and benzene. The obtained values for activation energies and rate constants, in both solvents, are in excellent agreement with thermodynamic results (Marino et al., 2014), namely, kinetic data for the investigated compound indicating position C1 as the most reactive one.

When the total rate constants are calculated for the reaction with •OH, the results show that the reactions of GA with this radical are diffusion limited. It is worth mentioning that the reactivity of GA toward •OH is more heterogeneous for different mechanisms and reaction positions. In addition, all mechanical pathways play a significant role in total reactivity, n nonpolar media. There is only one exception, in the case where the reaction takes place by the RAF mechanism in position 4. Based on a separate analysis of the HAT and RAF mechanisms, it can be concluded that the contribution of the HAT mechanism is greater than the contribution of the RAF mechanism. On the other hand, taking into account all reaction pathways for HAT and RAF mechanism, it is evident that both of them have important role in the scavenging activity of •OH with GA. The SPLET mechanism becomes the major reaction path, at physiological pH, in aqueous solution.

10.1 Electron-transfer reaction of quercetin

According to Marcus' approach, the important parameters for the investigation of the electron-transfer reactions are the changes of the reaction in Gibbs free energy, reorganizational energy, and diffusion rate constant. The free radical-scavenging activities of Q were also studied via the second step of SPLET mechanism, electron transfer. For this research study, molecular simulation was performed in water, as polar solvent. The calculated values of the electron-transfer reactions in the second step of SPLET are presented in Table 7.9.

It is evident from Table 7.9 that reaction Gibbs energy change is negative. When the apparent rate constant is corrected for diffusion, the values of the electron-transfer rate constants are of the order of magnitude 10^9. The 3-OH group of Q has the lowest value of free energy

Table 7.9 [a]Results related to electron transfer from the 3, 3′, and 4′ positions of Q^- to $HO^\bullet$ in water, at the M062X/6-311 ++G(d,p) level of theory.

Position	ΔG_{ET}° (kJ mol^{-1})	λ (kJ mol^{-1})	k_{ET} (M^{-1} s^{-1})	k_{app} (M^{-1} s^{-1})
3	− 80.8	78.6	6.17×10^{12}	4.14×10^{9}
3′	− 69.3	65.7	6.09×10^{12}	4.10×10^{9}
4′	− 66.9	62.8	6.05×10^{12}	5.87×10^{9}

[a]ΔG_{ET}° and λ denote free energy of reaction and reorganization energy, whereas k_{ET} and k_{app} stand for rate constant arising from TST, rate constant for an irreversible bimolecular and apparent rate constant, respectively.

change for the reaction with hydroxyl radical in water. This result implies 3-OH group as the most favorable position for the reaction via electron-transfer mechanism (ET). In addition, thermochemical and kinetic analyses are in agreement and also show good compatibility with our previous results.

10.2 Electron-transfer mechanism of GA

Kinetic parameters of free radical-scavenging activity of GA were calculated by using three different radicals: $^\bullet OH$, $CH_3OO^\bullet$, and $^\bullet OOH$ (Fig. 7.11). The thermochemical parameters of the reactions between selected radicals and GA were analyzed in terms of their Gibbs free energies.

The free radical-scavenging activities of gallic acid were studied via electron transfer, the second step of SPLET mechanism (Table 7.10). The molecular simulation was performed in water and pentyl ethanoate as solvents. Some thermochemical and kinetic data for reactions of gallic acid molecule with three different free radicals are calculated (Đorović et al., 2015). In water, the most favorable reaction is with hydroxyl radical. In the second place is the reaction with hydroperoxyl radical, and the least possible is the reaction with methylperoxyl radical, which is lipid peroxyl radical. Value of the activation energy for reaction with $^\bullet OH$ radical is slightly lower for position 3 of GA molecule, while values of the activation energies for reaction with other two radicals are somewhat lower for position 4. Free energies of reactions are in agreement with activation energies and are comparable with rate constants of the examined reactions. When the values of activation energies are lower, the corresponding values of rate constants are higher, and possible reaction is

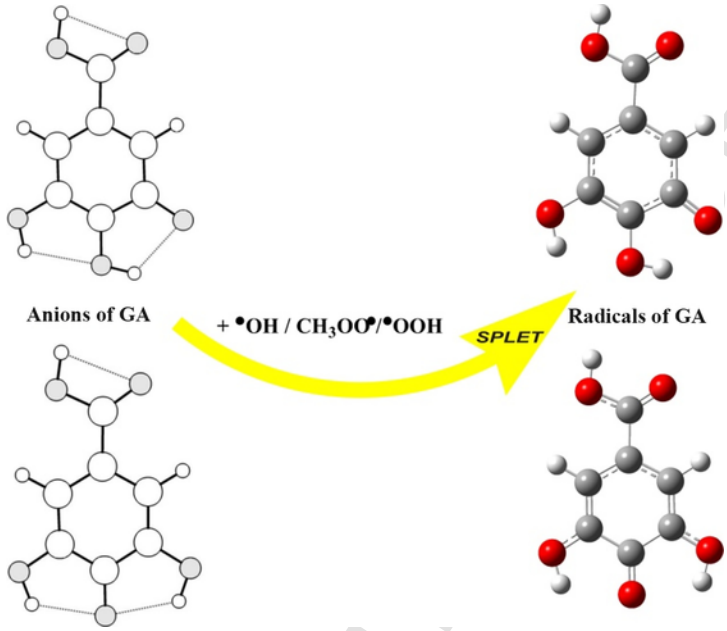

Fig. 7.11 General scheme of the examined reactions.

Table 7.10 DFT calculations of rate constants related to SPLET mechanism.

Gallic acid	$\Delta G^{\ddagger}_{SPLET}$ (kJ mol^{-1})	ΔG^{0}_{SPLET} (kJ mol^{-1})	λ (kJ mol^{-1})	k_d (M^{-1} s^{-1})	k_{app} (M^{-1} s^{-1})
Water ε = 78.35					
3 +•OH	21.5	− 60.6	19.6	8.06×10^{9}	9.6×10^{8}
3 + $CH_3OO^{\bullet}$	73.4	46.0	190.7	6.68×10^{9}	8.4×10^{-1}
3 +•OOH	63.1	37.6	169.0	7.21×10^{9}	5.4×10^{1}
4 +•OH	22.6	− 62.9	20.2	8.22×10^{9}	6.2×10^{8}
4 + $CH_3OO^{\bullet}$	71.6	43.4	189.8	6.84×10^{9}	1.7
4 +•OOH	61.6	35.3	168.3	7.37×10^{9}	1.0×10^{2}
Pentyl ethanoate ε = 4.73					
3 +•OH	29.4	23.7	61.1	8.44×10^{9}	4.4×10^{7}
3 + $CH_3OO^{\bullet}$	137.5	118.6	258.3	7.13×10^{9}	4.4×10^{-12}
3 +•OOH	128.3	111.4	238.3	7.79×10^{9}	2.1×10^{-10}
4 +•OH	17.9	24.7	57.2	8.12×10^{9}	2.8×10^{8}
4 + $CH_3OO^{\bullet}$	112.8	132.5	254.4	7.08×10^{9}	3.8×10^{-11}
4 +•OOH	105.6	123.3	234.4	7.74×10^{9}	1.5×10^{-9}

faster. Similar results are obtained in pentyl ethanoate with difference in the lowest values of activation energy in reaction with hydroxyl radical. The pentyl ethanoate is used to mimic lipid environment (Pérez-González et al., 2014). In general, thermochemical and kinetic analyses are in agreement and also show good compatibility with our previous results (Table 7.10).

11 CONCLUSION

OS is a disbalance of the oxidoreduction processes in the organism and is caused with the excessive production of free radicals. Antioxidants can prevent cell damage induced by oxidants. Antioxidative protection is a very complex process and can be investigated using both experimental (in vivo or in vitro) and theoretical (in silico) approaches; albeit combined studies are probably the best choice. The most common computational strategies used for that purpose include those based on reactivity, thermochemical, and kinetic data. The antiradical properties of antioxidants are based on their ability to donate hydrogen atom to a free radical species. In these reactions, newly formed radical is generated from antioxidant molecule, and that new formed species is more stable and less reactive than the initial free radical. There are numerous mechanisms of the antioxidant actions of free radicals, and the most studied are hydrogen atom transfer (HAT), single-electron transfer followed by proton transfer (SET-PT), and sequential proton loss electron transfer (SPLET). Antioxidant activity can be determined on the basis of the calculated thermodynamic properties of the parent molecules and the corresponding radicals, radical cations, and anions. BDE, PA, and IP values serve to confirm thermodynamically most favorable reaction pathway. The HAT mechanism is the most favorable reaction pathway for antioxidative action in nonpolar solvents. On the other hand, the SPLET mechanism is the most preferable reaction pathway for antioxidative action in water, as the polar solution. The IP values for all investigated molecules are notably high. For this reason, it has been generally accepted that SET-PT is not a plausible mechanism for investigated compounds. These facts are confirmed in the case of all examined compounds presented in this chapter. The antiradical mechanisms of the inactivation of free radical species have also been estimated on the bases of the values of reaction enthalpies related to

HAT, SPLET, and SET-PT mechanisms. The influence of free radical species is also taken into account. This approach is used to verify results achieved with the standard thermodynamic approach previously mentioned. Good consistency has been achieved with results obtained with the standard procedure. At the end, antioxidative action can be examined using the kinetics of reactions. The mechanistic approach is applied as affirmation of results obtained with previously mentioned thermodynamical approaches. In general, thermodynamic and kinetic studies are in agreement.

REFERENCES

Alberty, R.A., Hammes, G.G., 1958. Application of the theory of diffusion-controlled reactions to enzyme kinetics. J. Phys. Chem. 62 (2), 154–159.

Anouar, E., Calliste, C.A., Kosinova, P., Di Meo, F., Duroux, J.L., Champavier, Y., Marakchi, K., Trouillas, P., 2009. Free radical scavenging properties of guaiacol oligomers: a combined experimental and quantum study of the guaiacyl-moiety role. J. Phys. Chem. A 113 (50), 13881–13891.

Augustyniak, A., Bartosz, G., Čipak, A., Duburs, G., Horáková, L.U., Łuczaj, W., Majekova, M., Odysseos, A.D., Rackova, L., Skrzydlewska, E., Stefek, M., 2010. Natural and synthetic antioxidants: an updated overview. Free Radic. Res. 44 (10), 1216–1262.

Barzegar, A., 2012. The role of electron-transfer and H-atom donation on the superb antioxidant activity and free radical reaction of curcumin. Food Chem. 135 (3), 1369–1376.

Benavente-García, O., Castillo, J., Marin, F.R., Ortuño, A., Del Río, J.A., 1997. Uses and properties of citrus flavonoids. J. Agric. Food Chem. 45 (12), 4505–4515.

Bianco, M.A., Handaji, A., Savolainen, H., 1998. Quantitative analysis of ellagic acid in hardwood samples. Sci. Total Environ. 222 (1-2), 123–126.

Block, G., Patterson, B., Subar, A., 1992. Fruit, vegetables, and cancer prevention: a review of the epidemiological evidence. Nutr. Cancer 18 (1), 1–29.

Bors, W., Heller, W., Michel, C., Saran, M., 1990. Flavonoids as antioxidants: determination of radical-scavenging efficiencies. In: Methods in Enzymology. vol. 186, Academic Press, pp. 343–355.

Bugg, T.D., 2003. Dioxygenase enzymes: catalytic mechanisms and chemical models. Tetrahedron 59 (36), 7075–7101.

Burton, G.W., Ingold, K.U., 1984. Beta-carotene: an unusual type of lipid antioxidant. Science 224 (4649), 569–573.

Cai, Y.Z., Sun, M., Xing, J., Luo, Q., Corke, H., 2006. Structure–radical scavenging activity relationships of phenolic compounds from traditional Chinese medicinal plants. Life Sci. 78 (25), 2872–2888.

Cao, G., Sofic, E., Prior, R.L., 1997. Antioxidant and prooxidant behavior of flavonoids: structure-activity relationships. Free Radic. Biol. Med. 22 (5), 749–760.

Carpenter, J.E., Weinhold, F., 1988. Analysis of the geometry of the hydroxymethyl radical by the "different hybrids for different spins" natural bond orbital procedure. J. Mol. Struct. Theochem. 169, 41–62.

Chao, C.Y., Yin, M.C., 2009. Antibacterial effects of roselle calyx extracts and protocatechuic acid in ground beef and apple juice. Foodborne Pathog. Dis. 6 (2), 201–206.

Chatgilialoglu, C., D'Angelantonio, M., Guerra, M., Kaloudis, P., Mulazzani, Q.G., 2009. A reevaluation of the ambident reactivity of the guanine moiety towards hydroxyl radicals. Angew. Chem. Int. Ed. 48 (12), 2214–2217.

Collins, F.C., Kimball, G.E., 1949. Diffusion-controlled reaction rates. J. Colloid Sci. 4 (4), 425–437.

Day, A.J., Cañada, F.J., Díaz, J.C., Kroon, P.A., Mclauchlan, R., Faulds, C.B., Plumb, G.W., Morgan, M.R., Williamson, G., 2000. Dietary flavonoid and isoflavone glycosides are hydrolysed by the lactase site of lactase phlorizin hydrolase. FEBS Lett. 468 (2-3), 166–170.

De Graff, W.G., Myers, L.S., Mitchell, J.B., Hahn, S.M., 2003. Protection against Adriamycin® cytotoxicity and inhibition of DNA topoisomerase II activity by 3, 4-dihydroxybenzoic acid. Int. J. Oncol. 23 (1), 159–163.

Dhaouadi, Z., Nsangou, M., Garrab, N., Anouar, E.H., Marakchi, K., Lahmar, S., 2009. DFT study of the reaction of quercetin with· O2-and· OH radicals. J. Mol. Struct. Theochem. 904 (1-3), 35–42.

DiLabio, G.A., Johnson, E.R., 2007. Lone pair–π and π–π interactions play an important role in proton-coupled electron transfer reactions. J. Am. Chem. Soc. 129 (19), 6199–6203.

Dimić, D., Milenković, D., Marković, J.D., Marković, Z., 2017. Antiradical activity of catecholamines and metabolites of dopamine: theoretical and experimental study. Phys. Chem. Chem. Phys. 19 (20), 12970–12980.

Đorović, J., Marković, J.M.D., Stepanić, V., Begović, N., Amić, D., Marković, Z., 2014. Influence of different free radicals on scavenging potency of gallic acid. J. Mol. Model. 20 (7), 2345.

Đorović, J.R., Milenković, D.A., Marković, Z.S., 2015. Study of electron transfer mechanism of gallic acid. In: 2015 IEEE 15th International Conference on Bioinformatics and Bioengineering (BIBE). IEEE, pp. 1–5.

Douki, T., Cadet, J., 1996. Peroxynitrite mediated oxidation of purine bases of nucleosides and isolated DNA. Free Radic. Res. 24 (5), 369–380.

Duncan, W.T., Bell, R.L., Truong, T.N., 1998. TheRate: Program for ab initio direct dynamics calculations of thermal and vibrational-state-selected rate constants. J. Comput. Chem. 19 (9), 1039–1052.

Eigen, M., Hammes, G.G., 2006. Elementary steps in enzyme reactions (as studied by relaxation spectrometry). Adv. Enzymol. Relat. Areas Mol. Biol. 25, 1–38.

Estévez, L., Otero, N., Mosquera, R.A., 2010. A computational study on the acidity dependence of radical-scavenging mechanisms of anthocyanidins. J. Phys. Chem. B 114 (29), 9706–9712.

Foti, M.C., 2007. Antioxidant properties of phenols. J. Pharm. Pharmacol. 59 (12), 1673–1685.

Fridovich, I., 1978. The biology of oxygen radicals. Science 201 (4359), 875–880.

Galano, A., 2011. On the direct scavenging activity of melatonin towards hydroxyl and a series of peroxyl radicals. Phys. Chem. Chem. Phys. 13 (15), 7178–7188.

Galano, A., 2015. Free radicals induced oxidative stress at a molecular level: the current status, challenges and perspectives of computational chemistry based protocols. J. Mex. Chem. Soc. 59 (4), 231–262.

Galano, A., Alvarez-Idaboy, J.R., 2009. Guanosine + OH radical reaction in aqueous solution: a reinterpretation of the UV–vis data based on thermodynamic and kinetic calculations. Org. Lett. 11 (22), 5114–5117.

Galano, A., Alvarez-Idaboy, J.R., 2013. A computational methodology for accurate predictions of rate constants in solution: application to the assessment of primary antioxidant activity. J. Comput. Chem. 34 (28), 2430–2445.
Galano, A., Francisco Marquez, M., Pérez-González, A., 2014. Ellagic acid: an unusually versatile protector against oxidative stress. Chem. Res. Toxicol. 27 (5), 904–918.
Galano, A., Francisco-Marquez, M., 2009. Reactions of OOH radical with β-carotene, lycopene, and torulene: hydrogen atom transfer and adduct formation mechanisms. J. Phys. Chem. B 113 (32), 11338–11345.
Galano, A., Mazzone, G., Alvarez-Diduk, R., Marino, T., Alvarez-Idaboy, J.R., Russo, N., 2016. Food antioxidants: chemical insights at the molecular level. Annu. Rev. Food Sci. Technol. 7, 335–352.
Galano, A., Vargas, R., Martínez, A., 2010. Carotenoids can act as antioxidants by oxidizing the superoxide radical anion. Phys. Chem. Chem. Phys. 12 (1), 193–200.
Halliwell, B., 2005. Free Radicals and Other Reactive Species in Disease. eLS.
Halliwell, B., Aeschbach, R., Löliger, J., Aruoma, O.I., 1995. The characterization of antioxidants. Food Chem. Toxicol. 33 (7), 601–617.
Halliwell, B., Gutteridge, J.M., 2015. Free Radicals in Biology and Medicine. Oxford University Press, USA.
Havsteen, B., 1983. Flavonoids, a class of natural products of high pharmacological potency. Biochem. Pharmacol. 32 (7), 1141–1148.
Hertog, M.G., Hollman, P.C., 1996. Potential health effects of the dietary flavonol quercetin. Eur. J. Chem. Nutr. 50, 63–71.
Hill, T.J., Land, E.J., McGarvey, D.J., Schalch, W., Tinkler, J.H., Truscott, T.G., 1995. Interactions between carotenoids and the CCl3O2.bul.Radical. J. Am. Chem. Soc. 117 (32), 8322–8326.
Hollman, P.C., 2004. Absorption, bioavailability, and metabolism of flavonoids. Pharm. Boil. 42 (1), 74–83.
Huang, M.T., Ferraro, T., 1992. Phenolic compounds in food and cancer prevention. In: Phenolic Compounds in Food and Their Effects on Health. II. Antioxidants and Cancer PreVention. American Chemical Society, Washington, DC, pp. 8–34.
Inagaki, T., Yamamoto, T., 2014. Critical role of deep hydrogen tunneling to accelerate the antioxidant reaction of ubiquinol and vitamin E. J. Phys. Chem. B 118 (4), 937–950.
Ivanović, N., Jovanović, L., Marković, Z., Marković, V., Joksović, M.D., Milenković, D., Djurdjević, P.T., Ćirić, A., Joksović, L., 2016. Potent 1, 2, 4-triazole-3-thione radical scavengers derived from phenolic acids: synthesis, electrochemistry, and theoretical study. ChemistrySelect 1 (13), 3870–3878.
Jacob, R.A., Burri, B.J., 1996. Oxidative damage and defense. Am. J. Clin. Nutr. 63 (6), 985S–990S.
Jeremić, S., Filipović, N., Peulić, A., Marković, Z., 2014. Thermodynamical aspect of radical scavenging activity of alizarin and alizarin red S. Theoretical comparative study. Comput. Theor. Chem. 1047, 15–21.
Jeremić, S.R., Šehović, S.F., Manojlović, N.T., Marković, Z.S., 2012. Antioxidant and free radical scavenging activity of purpurin. Monatsh. Chem. 143 (3), 427–435.
Kaul, T.N., Middleton, E., Ogra, P.L., 1985. Antiviral effect of flavonoids on human viruses. J. Med. Virol. 15 (1), 71–79.
Kim, D.O., Lee, C.Y., 2004. Comprehensive study on vitamin C equivalent antioxidant capacity (VCEAC) of various polyphenolics in scavenging a free radical and its structural relationship. Crit. Rev. Food Sci. Nutr. 44 (4), 253–273.
Klein, E., Lukeš, V., Ilčin, M., 2007. DFT/B3LYP study of tocopherols and chromans antioxidant action energetics. Chem. Phys. 336 (1), 51–57.

Koga, T., Moro, K., Nakamori, K., Yamakoshi, J., Hosoyama, H., Kataoka, S., Ariga, T., 1999. Increase of antioxidative potential of rat plasma by oral administration of proanthocyanidin-rich extract from grape seeds. J. Agric. Food Chem. 47 (5), 1892–1897.

Kwon, Y.I.I., Vattem, D.A., Shetty, K., 2006. Evaluation of clonal herbs of Lamiaceae species for management of diabetes and hypertension. Asia Pac. J. Clin. Nutr. 15 (1), 107–118.

León-Carmona, J.R., Alvarez-Idaboy, J.R., Galano, A., 2012. On the peroxyl scavenging activity of hydroxycinnamic acid derivatives: mechanisms, kinetics, and importance of the acid–base equilibrium. Phys. Chem. Chem. Phys. 14 (36), 12534–12543.

Lin, C.Y., Huang, C.S., Huang, C.Y., Yin, M.C., 2009. Anticoagulatory, antiinflammatory, and antioxidative effects of protocatechuic acid in diabetic mice. J. Agric. Food Chem. 57 (15), 6661–6667.

Litwinienko, G., Ingold, K.U., 2007. Solvent effects on the rates and mechanisms of reaction of phenols with free radicals. Acc. Chem. Res. 40 (3), 222–230.

Marcus, R.A., 1964. Chemical and electrochemical electron-transfer theory. Annu. Rev. Phys. Chem. 15 (1), 155–196.

Marcus, R.A., 1997. Transfer reactions in chemistry. Theory and experiment. Pure Appl. Chem. 69 (1), 13–30.

Marenich, A.V., Cramer, C.J., Truhlar, D.G., 2009. Performance of SM6, SM8, and SMD on the SAMPL1 test set for the prediction of small-molecule solvation free energies. J. Phys. Chem. B 113 (14), 4538–4543.

Marino, T., Galano, A., Russo, N., 2014. Radical scavenging ability of gallic acid toward OH and OOH radicals. Reaction mechanism and rate constants from the density functional theory. J. Phys. Chem. B 118 (35), 10380–10389.

Marković, Z., Amić, D., Milenković, D., Dimitrić-Marković, J.M., Marković, S., 2013. Examination of the chemical behavior of the quercetin radical cation towards some bases. Phys. Chem. Chem. Phys. 15 (19), 7370–7378.

Marković, Z., Đorović, J., Dekić, M., Radulović, M., Marković, S., Ilić, M., 2013. DFT study of free radical scavenging activity of erodiol. Chem. Pap. 67 (11), 1453–1461.

Marković, Z., Đorović, J., Marković, J.M.D., Živić, M., Amić, D., 2014. Investigation of the radical scavenging potency of hydroxybenzoic acids and their carboxylate anions. Monatsh. Chem. 145 (6), 953–962.

Marković, Z.S., Marković, S., Dimitrić Marković, J.M., Milenković, D., 2012. Structure and reactivity of baicalein radical cation. Int. J. Quantum Chem. 112 (8), 2009–2017.

Marković, Z.S., Marković, J.M.D., Doličanin, Ć.B., 2010. Mechanistic pathways for the reaction of quercetin with hydroperoxy radical. Theor. Chem. Accounts 127 (1-2), 69–80.

Marković, J.M.D., Milenković, D., Amić, D., Mojović, M., Pašti, I., Marković, Z.S., 2014. The preferred radical scavenging mechanisms of fisetin and baicalein towards oxygen-centred radicals in polar protic and polar aprotic solvents. RSC Adv. 4 (61), 32228–32236.

Marković, J.M.D., Milenković, D., Amić, D., Popović-Bijelić, A., Mojović, M., Pašti, I.A., Marković, Z.S., 2014. Energy requirements of the reactions of kaempferol and selected radical species in different media: towards the prediction of the possible radical scavenging mechanisms. Struct. Chem. 25 (6), 1795–1804.

Marković, Z., Milenković, D., Đorović, J., Jeremić, S., 2013. Solvation enthalpies of the proton and electron in polar and non-polar solvents. JSSCM 7 (2), 1–9.

Marković, Z., Milenković, D., Đorović, J., Marković, J.M.D., Stepanić, V., Lučić, B., Amić, D., 2012. PM6 and DFT study of free radical scavenging activity of morin. Food Chem. 134 (4), 1754–1760.

Marković, Z., Milenković, D., Đorović, J., Marković, J.M.D., Stepanić, V., Lučić, B., Amić, D., 2012. Free radical scavenging activity of morin 2′-O − phenoxide anion. Food Chem. 135 (3), 2070–2077.
Marković, Z., Tošović, J., Milenković, D., Marković, S., 2016. Revisiting the solvation enthalpies and free energies of the proton and electron in various solvents. Comput. Theor. Chem. 1077, 11–17.
Martínez, A., Galano, A., Vargas, R., 2011. Free radical scavenger properties of α-mangostin: thermodynamics and kinetics of HAT and RAF mechanisms. J. Phys. Chem. B 115 (43), 12591–12598.
Martínez, A., Hernández-Marin, E., Galano, A., 2012. Xanthones as antioxidants: a theoretical study on the thermodynamics and kinetics of the single electron transfer mechanism. Food Funct. 3 (4), 442–450.
Mayer, J.M., 2004. Proton-coupled electron transfer: a reaction chemist's view. Annu. Rev. Phys. Chem. 55, 363–390.
Mayer, J.M., Hrovat, D.A., Thomas, J.L., Borden, W.T., 2002. Proton-coupled electron transfer versus hydrogen atom transfer in benzyl/toluene, methoxyl/methanol, and phenoxyl/phenol self-exchange reactions. J. Am. Chem. Soc. 124 (37), 11142–11147.
Mazzone, G., Galano, A., Alvarez-Idaboy, J.R., Russo, N., 2016. Coumarin–Chalcone hybrids as peroxyl radical scavengers: kinetics and mechanisms. J. Chem. Inf. Model. 56 (4), 662–670.
Medina, M.E., Galano, A., Alvarez-Idaboy, J.R., 2014. Theoretical study on the peroxyl radicals scavenging activity of esculetin and its regeneration in aqueous solution. Phys. Chem. Chem. Phys. 16 (3), 1197–1207.
Medina, M.E., Iuga, C., Alvarez-Idaboy, J.R., 2013. Antioxidant activity of propyl gallate in aqueous and lipid media: a theoretical study. Phys. Chem. Chem. Phys. 15 (31), 13137–13146.
Milenković, D., Đorović, J., Jeremić, S., Dimitrić Marković, J.M., Avdović, E.H., Marković, Z., 2017. Free radical scavenging potency of dihydroxybenzoic acids. J. Chem. 2017.
Min, D.B., Boff, J.M., 2002. Chemistry and reaction of singlet oxygen in foods. Compr. Rev. Food Sci. Food Saf. 1 (2), 58–72.
Mortensen, A., Skibsted, L.H., Sampson, J., Rice-Evans, C., Everett, S.A., 1997. Comparative mechanisms and rates of free radical scavenging by carotenoid antioxidants. FEBS Lett. 418 (1-2), 91–97.
Musialik, M., Kuzmicz, R., Pawłowski, T.S., Litwinienko, G., 2009. Acidity of hydroxyl groups: an overlooked influence on antiradical properties of flavonoids. J. Org. Chem. 74 (7), 2699–2709.
Nakanishi, I., Ohkubo, K., Miyazaki, K., Hakamata, W., Urano, S., Ozawa, T., Okuda, H., Fukuzumi, S., Ikota, N., Fukuhara, K., 2004. A planar catechin analogue having a more negative oxidation potential than (+)-catechin as an electron transfer antioxidant against a peroxyl radical. Chem. Res. Toxicol. 17 (1), 26–31.
Nakanishi, I., Shimada, T., Ohkubo, K., Manda, S., Shimizu, T., Urano, S., Okuda, H., Miyata, N., Ozawa, T., Anzai, K., Fukuzumi, S., 2007. Involvement of electron transfer in the radical-scavenging reaction of resveratrol. Chem. Lett. 36 (10), 1276–1277.
Nelsen, S.F., Blackstock, S.C., Kim, Y., 1987. Estimation of inner shell Marcus terms for amino nitrogen compounds by molecular orbital calculations. J. Am. Chem. Soc. 109 (3), 677–682.
Ness, A.R., Powles, J.W., 1997. Fruit and vegetables, and cardiovascular disease: a review. Int. J. Epidemiol. 26 (1), 1–13.
Neta, P., Huie, R.E., Mosseri, S., Shastri, L.V., Mittal, J.P., Maruthamuthu, P., Steenken, S., 1989. Rate constants for reduction of substituted methylperoxyl radicals by

ascorbate ions and N, N, N', N'-tetramethyl-p-phenylenediamine. J. Phys. Chem. 93 (10), 4099–4104.
Pérez-González, A., Galano, A., 2012. On the outstanding antioxidant capacity of edaravone derivatives through single electron transfer reactions. J. Phys. Chem. B 116 (3), 1180–1188.
Pérez-González, A., Galano, A., Alvarez-Idaboy, J.R., 2014. Dihydroxybenzoic acids as free radical scavengers: mechanisms, kinetics, and trends in activity. New J. Chem. 38 (6), 2639–2652.
Petrović, Z.D., Đorović, J., Simijonović, D., Petrović, V.P., Marković, Z., 2015. Experimental and theoretical study of antioxidative properties of some salicylaldehyde and vanillic Schiff bases. RSC Adv. 5 (31), 24094–24100.
Pettersen, R.C., Ward, J.C., Lawrence, A.H., 1993. Detection of northern red oak wetwood by fast heating and ion mobility spectrometric analysis. Holzforschung 47 (6), 513–522.
Prasad, K., Laxdal, V.A., 1994. Hydroxyl radical-scavenging property of indomethacin. Mol. Cell. Biochem. 136 (2), 139–144.
Prütz, W.A., Mönig, H., Butler, J., Land, E.J., 1985. Reactions of nitrogen dioxide in aqueous model systems: oxidation of tyrosine units in peptides and proteins. Arch. Biochem. Biophys. 243 (1), 125–134.
Pryor, W.A., 1986. Oxy-radicals and related species: their formation, lifetimes, and reactions. Annu. Rev. Physiol. 48 (1), 657–667.
Pryor, W.A., 1988. Why is the hydroxyl radical the only radical that commonly adds to DNA? Hypothesis: it has a rare combination of high electrophilicity, high thermochemical reactivity, and a mode of production that can occur near DNA. Free Radic. Biol. Med. 4 (4), 219–223.
Radi, R., Peluffo, G., Alvarez, M.N., Naviliat, M., Cayota, A., 2005. Unraveling peroxynitrite formation in biological systems. Free Radic. Biol. Med. 39 (10), 1286.
Rice-Evans, C.A., Miller, N.J., 1996. Antioxidant activities of flavonoids as bioactive components of food. Biochem. Soc. Trans. 24, 790–795.
Rice-Evans, C.A., Miller, N.J., Paganga, G., 1996. Structure-antioxidant activity relationships of flavonoids and phenolic acids. Free Radic. Biol. Med. 20 (7), 933–956.
Rose, R.C., Bode, A.M., 1993. Biology of free radical scavengers: an evaluation of ascorbate. FASEB J. 7 (12), 1135–1142.
Sakagami, H., Yokote, Y., Akahane, K., 2001. Changes in amino acid pool and utilization during apoptosis in HL-60 cells induced by epigallocatechin gallate or gallic acid. Anticancer Res. 21 (4A), 2441–2447.
Sies, H., 1997. Oxidative stress: oxidants and antioxidants. Exp. Physiol. 82 (2), 291–295.
Smoluchowski, M.V., 1918. Versuch einer mathematischen Theorie der Koagulationskinetik kolloider Lösungen. Z. Phys. Chem. 92 (1), 129–168.
Squadrito, G.L., Pryor, W.A., 1998. Oxidative chemistry of nitric oxide: the roles of superoxide, peroxynitrite, and carbon dioxide. Free Radic. Biol. Med. 25 (4-5), 392–403.
Stagos, D., Kazantzoglou, G., Theofanidou, D., Kakalopoulou, G., Magiatis, P., Mitaku, S., Kouretas, D., 2006. Activity of grape extracts from Greek varieties of Vitis vinifera against mutagenicity induced by bleomycin and hydrogen peroxide in Salmonella typhimurium strain TA102. Mutat. Res. 609 (2), 165–175.
Stokes, S.G.G., 1903. Mathematical and Physical Papers. vol. 3, Cambridge University Press, Cambridge, esp. Sect. IV, 55.
Sueishi, Y., Hori, M., Kita, M., Kotake, Y., 2011. Nitric oxide (NO) scavenging capacity of natural antioxidants. Food Chem. 129 (3), 866–870.

Thomas, C., 1998. Oxygen Radicals and the Disease Process. CRC Press.
Tošović, J., Marković, S., Marković, J.M.D., Mojović, M., Milenković, D., 2017. Antioxidative mechanisms in chlorogenic acid. Food Chem. 237, 390–398.
Van Dorsten, F.A., Peters, S., Gross, G., Gomez-Roldan, V., Klinkenberg, M., De Vos, R.C., Vaughan, E.E., Van Duynhoven, J.P., Possemiers, S., Van de Wiele, T., Jacobs, D.M., 2012. Gut microbial metabolism of polyphenols from black tea and red wine/grape juice is source-specific and colon-region dependent. J. Agric. Food Chem. 60 (45), 11331–11342.
Xie, J., Schaich, K.M., 2014. Re-evaluation of the 2, 2-diphenyl-1-picrylhydrazyl free radical (DPPH) assay for antioxidant activity. J. Agric. Food Chem. 62 (19), 4251–4260.
Yan, X.T., Lee, S.H., Li, W., Sun, Y.N., Yang, S.Y., Jang, H.D., Kim, Y.H., 2014. Evaluation of the antioxidant and anti-osteoporosis activities of chemical constituents of the fruits of Prunus mume. Food Chem. 156, 408–415.

FURTHER READING

Glendening, E.D., Badenhoop, J.K., Reed, A.E., Carpenter, J.E., Bohmann, J.A., Morales, C.M., Weinhold, F., 2004. NBO 5.0; Theoretical Chemistry Institute, University of Wisconsin: Madison, WI, 2001.
Milenković, D., Đorović, J., Petrović, V., Avdović, E., Marković, Z., 2018. Hydrogen atom transfer versus proton coupled electron transfer mechanism of gallic acid with different peroxy radicals. React. Kinet. Mech. Catal. 123 (1), 215–230.
Reiter, R.J., Tan, D.X., Herman, T.S., Thomas, C.R., 2004. Melatonin as a radioprotective agent: a review. Int. J. Radiat. Oncol. Biol. Phys. 59 (3), 639–653.